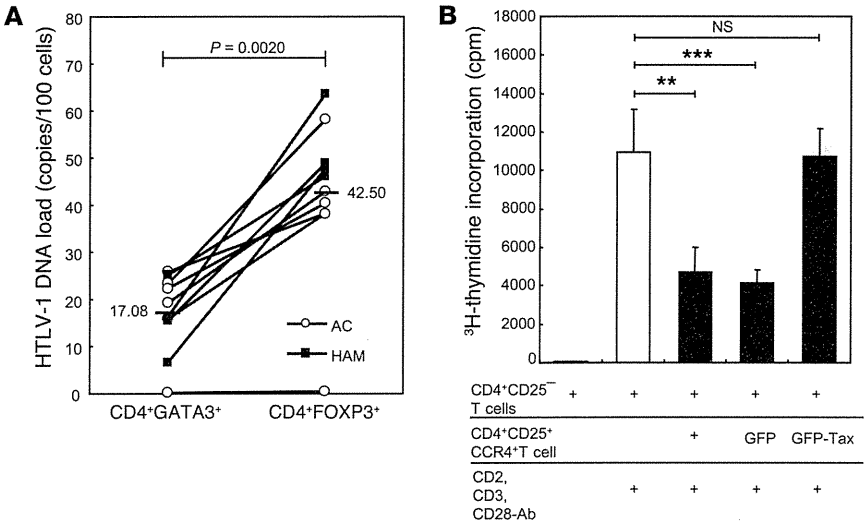

Figure 1. HTLV-1 mainly infects Tregs and inhibits their regulatory function. (**A**) Higher HTLV-1 proviral DNA load in $CD4^+FOXP3^+$ cells (Tregs) compared with $CD4^+GATA3^+$ cells ($P = 0.0020$, Wilcoxon test) from asymptomatic carriers (AC; $n = 6$) and HAM/TSP patients ($n = 4$). PBMCs were FACS sorted, and proviral load was measured using quantitative PCR. Horizontal bars represent the mean value for each set. (**B**) Loss of regulatory function in Tax-expressing $CD4^+CD25^+CCR4^+$ cells (Tregs). $CD4^+CD25^-$ T cells from an HD were stimulated with CD2, CD3, and CD28 antibodies and cultured alone or in the presence of equal numbers of $CD4^+CD25^+CCR4^+$ T cells, GFP lentivirus–infected HD $CD4^+CD25^+CCR4^+$ T cells, or GFP-Tax lentivirus–infected HD $CD4^+CD25^+CCR4^+$ T cells. As a control, $CD4^+CD25^-$ T cells alone were cultured without any stimulus. Proliferation of T cells was determined using ^{3}H-thymidine incorporation by adding ^{3}H-thymidine for 16 hours after 4 days of culture. All tests were performed in triplicate. Data are mean ± SD. $^{**}P < 0.01$, $^{***}P < 0.001$, ANOVA followed by Tukey test for multiple comparisons.

ease HTLV-1–associated myelopathy/tropical spastic paraparesis (HAM/TSP). The main other condition associated with the retrovirus is adult T cell leukemia/lymphoma (ATLL), a rare and aggressive cancer of the T cells. HAM/TSP represents a useful starting point from which to investigate the origins of chronic inflammation, because the primary cause of the disease — viral infection — is so unusually well defined. HAM/TSP patients share many immunological characteristics with FOXP3 mutant mice, including multiorgan lymphocytic infiltrates, overproduction of inflammatory cytokines, and spontaneous lymphoproliferation of cultured $CD4^+$ T cells (16–18). We and others have proposed that HTLV-1 preferentially infects $CD4^+CD25^+CCR4^+$ T cells, a group that includes Tregs (7, 19). Samples of $CD4^+CD25^+CCR4^+$ T cells isolated from HAM/TSP patients exhibited low FOXP3 expression as well as reduced production of suppressive cytokines and low overall suppressive ability — in fact, these $CD4^+CD25^+CCR4^+FOXP3^-$ T cells were shown to produce IFN-γ and express Ki67, a marker of cell proliferation (19). The frequency of these IFN-γ–producing $CD4^+CD25^+CCR4^+$ T cells in HAM/TSP patients was correlated with disease severity (19). Finally, evidence suggests that the HTLV-1 protein product Tax may play a role in this alleged transformation of Tregs into proinflammatory cells in HAM/TSP patients: transfecting Tax into $CD4^+CD25^+$ cells from healthy donors (HDs) reduced FOXP3 mRNA expression, and Tax expression in $CD4^+CD25^+CCR4^+$ cells was higher in HAM/TSP versus ATLL patients despite similar proviral loads (19, 20). Therefore, we hypothesized that HTLV-1 causes chronic inflammation by infecting $CD4^+CD25^+CCR4^+$ T cells and inducing their transformation into Th1-like, IFN-γ–producing proinflammatory cells via intracellular Tax expression and subsequent transcriptional alterations including but not limited to loss of endogenous FOXP3 expression.

In this study, we first sought to discover the detailed mechanism by which Tax influences the function of $CD4^+CD25^+CCR4^+$ T cells. We used DNA microarray analysis of $CD4^+CD25^+CCR4^+$ T cells from HAM/TSP patients to identify *TBX21*, known as a master transcription factor for Th1 differentiation, as a key intermediary between Tax expression and IFN-γ production. We demonstrated that Tax, in concert with specificity protein 1 (Sp1), amplified *TBX21* transcription and subsequently IFN-γ production. Next, we established the presence of Th1-like $CD4^+CCR4^+$ T cells in the CSF and spinal cord lesions of HAM/TSP patients. The majority of these $CD4^+CCR4^+$ T cells coexpressed CXCR3 as well as T-bet and IFN-γ. Finally, we investigated the therapeutic potential of an anti-CCR4 monoclonal antibody with antibody-dependent cellular cytotoxicity (ADCC) (21). Applying this antibody in vitro diminished the proliferative capacity of cultured PBMCs and reduced both proviral DNA load and IFN-γ production in cultured CSF cells as well as PBMCs. In conclusion, we were able to elucidate a more detailed mechanism for the pathogenesis of HAM/TSP and use our findings to suggest a possible therapeutic strategy.

Results

HTLV-1 preferentially infects Tregs and alters their behavior via Tax. Experiments were conducted to determine which among $CD4^+CD25^+CCR4^+$ T cells were infected by HTLV-1, and how the infection influenced their functionality. Analysis of fluorescence-activated cell sorting (FACS)-sorted PBMCs obtained from asymptomatic carriers ($n = 6$) as well as HAM/TSP patients ($n = 4$) revealed that Tregs ($CD4^+FOXP3^+$) carried much higher proviral loads than Th2 cells ($CD4^+GATA3^+$) ($P = 0.0020$; Figure 1A). As it is well established that each infected cell contains only 1 copy of the HTLV-1 provirus (22, 23), these results indicate that a larger proportion of $FOXP3^+$ than $GATA3^+$ $CD4^+$ T cells are infected. As expected, proliferation of $CD4^+CD25^-$ cells after stimulation, as measured by ^{3}H-thymidine incorporation, was suppressed upon coculture with $CD4^+CD25^+CCR4^+$ cells, including Tregs ($n = 3$, $P < 0.01$; Figure 1B). However, after being transduced with lentiviral vector expressing GFP-Tax, the $CD4^+CD25^+CCR4^+$ cells no longer suppressed cell proliferation; conversely, cells transduced with the control vector expressing only GFP retained full suppressive function ($P < 0.001$; Figure 1B).

The HTLV-1 protein product Tax induces IFN-γ production via T-bet. Experiments were conducted to determine if and how Tax affects IFN-γ production in infected T cells. First, the existence of a functional link between *Tax* and *IFNG* was established by using the

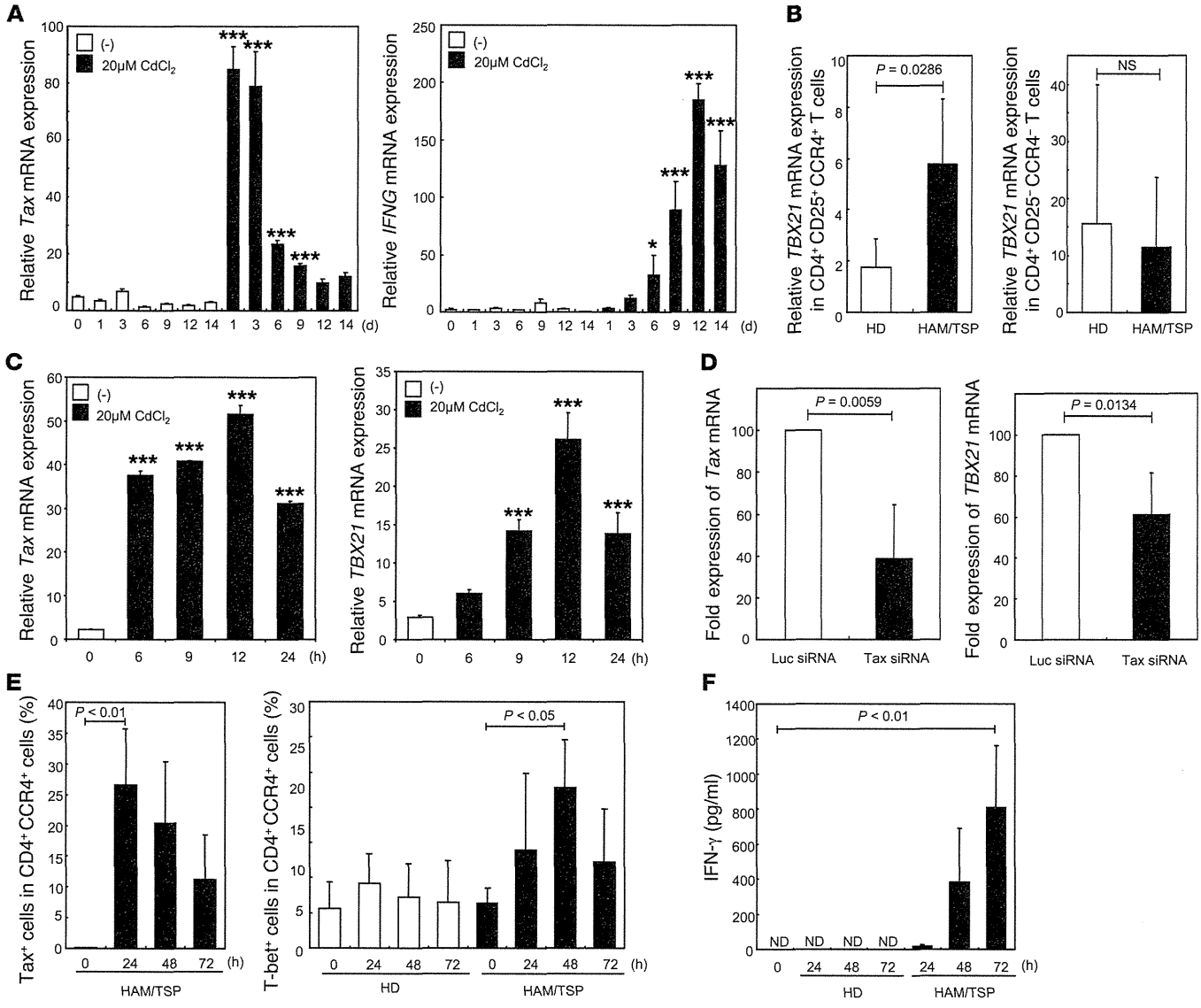

Figure 2. Tax induces IFN-γ production via T-bet. (**A**) Tax-dependent *IFNG* mRNA expression in JPX-9 cells. Experiments were performed in triplicate. (**B**) Elevated *TBX21* mRNA expression in $CD4^+CD25^+CCR4^+$ T cells from HAM/TSP patients relative to HDs (n = 4 per group). (**C**) Tax-dependent *TBX21* mRNA expression in JPX-9 cells. Experiments were performed in triplicate. (**D**) Reduced *TBX21* mRNA expression after silencing Tax in $CD4^+CD25^+CCR4^+$ T cells from HAM/TSP patients. PBMCs from HAM/TSP patients (n = 5) were FACS sorted, transfected with either Luc or Tax siRNA, and incubated for 24 hours. (**E** and **F**) Tax expression correlated with T-bet expression and IFN-γ production in $CD4^+CCR4^+$ T cells from HAM/TSP patients. $CD4^+CCR4^+$ T cells isolated from HDs and HAM/TSP patients (n = 4 per group) were cultured before being stained for Tax and T-bet protein and analyzed using FACS. IFN-γ production in the culture medium was measured using a CBA assay. ND, not detectable. All data are mean ± SD. P values were calculated using (**A** and **C**) 1-way ANOVA followed by Dunnett test for multiple comparisons, (**B**) Mann-Whitney U test, (**D**) paired t test, or (**E** and **F**) Friedman test followed by Dunn test for multiple comparisons. $^*P < 0.05$, $^{***}P < 0.001$ vs. time point 0.

JPX-9 cell line possessing a stably integrated $CdCl_2$-inducible *Tax* construct and measuring *IFNG* mRNA expression. Inducing *Tax* expression with $CdCl_2$ periodically over 2 weeks yielded a steady rise in *IFNG* expression (Figure 2A). Although there was clearly a correlation between Tax and IFN-γ expression, the *IFNG* expression level was not proportional to that of *Tax*, and the steepest rise in the former was delayed several days after the steepest rise in the latter. Thus, we suspected that expression of 1 or more additional genes may represent an important middle step on the pathway linking Tax and IFN-γ production. DNA microarray results revealed that expression of *TBX21*, which is known to be associated with IFN-γ production, was elevated in $CD4^+CD25^+CCR4^+$ cells from the HAM/TSP patient, but not the ATLL patient, compared with the HD (Supplemental Figure 1; supplemental material available online with this article; doi:10.1172/JCI75250DS1). *TBX21* mRNA expression, measured via real-time RT-PCR, was elevated in $CD4^+CD25^+CCR4^+$ cells, but not $CD4^+CD25^-CCR4^-$ cells, from HAM/TSP patients compared with HDs (Figure 2B). A direct correlation between *Tax* and *TBX21* mRNA expression was then established using the JPX-9 cell line, as described above (Figure 2C). Silencing the *Tax* gene with siRNA in $CD4^+CD25^+CCR4^+$ cells from HAM/TSP patients reduced *TBX21* as well as *Tax* expression (Figure 2D). Similarly,

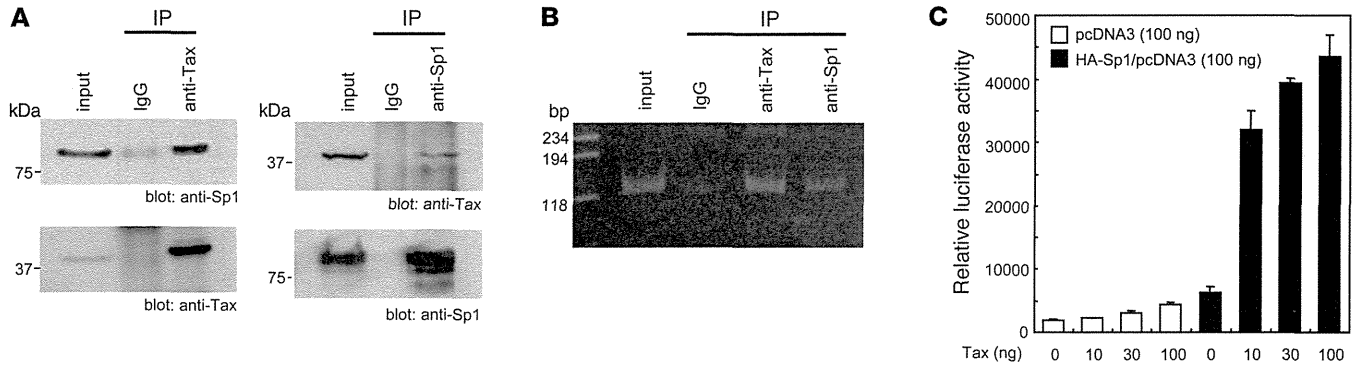

Figure 3. Tax and Sp1 cooperatively enhance *TBX21* promoter activity. (**A**) Co-IP of endogenous Tax and Sp1. Nuclear extracts from MT-2 cells were immunoprecipitated with anti-Tax or anti–Sp1 antibodies or with normal IgG as a control, then immunoblotted with anti-Tax or anti-Sp1 antibodies as indicated. (**B**) Tax bound to the *TBX21* promoter in vivo. ChIP assay using anti-Tax antibody followed by primers encompassing the *TBX21* promoter region (–179 to –59) was performed on genomic DNA isolated from MT-2 cells. DNA (input) and IP with anti-Sp1 served as positive controls, and normal IgG served as a negative control. (**C**) Coactivation of *TBX21* promoter by Sp1 and Tax. HEK293 cells were transfected with 100 ng of *TBX21*-Luc reporter plasmid or Sp1 expression plasmid, as well as 0–100 ng of Tax expression plasmid as indicated. Values were normalized to β-galactosidase activity as an internal control. Data are mean ± SD.

elevation of *Tax* expression via transduction of a GFP-Tax construct into $CD4^+CD25^+CCR4^+$ cells from a HD increased expression of *TBX21* as well as *Tax* (Supplemental Figure 2). Thus, a functional relationship between *Tax* and *TBX21* was confirmed. Finally, among $CD4^+CCR4^+$ cells from HAM/TSP patients, the appearance of Tax^+ cells was associated with a rise in the percentage of $T\text{-}bet^+$ cells, which was associated with a delayed but roughly proportional rise in the amount of IFN-γ protein (Figure 2, E and F). The production of Tax versus T-bet in these $CD4^+CCR4^+$ cells from HAM/TSP patients was compared at 0 versus 48 hours of culturing. At 0 hours, the overwhelming majority of the $CD4^+CCR4^+$ cells were both Tax^- and $T\text{-}bet^-$; by 48 hours, a substantial presence of $Tax^+T\text{-}bet^+$ cells had emerged, and there were very few $T\text{-}bet^+$ cells that were not also Tax^+ (Supplemental Figure 3).

Tax in concert with Sp1 induces TBX21 transcription. Experiments were conducted to investigate the mechanism by which Tax may be involved in *TBX21* transcription in HTLV-1–infected T cells. First, co-IP reactions were performed using nuclear extracts from the HTLV-1–infected MT-2 T cell line to confirm a suspected interaction between endogenous Tax and Sp1, which is known to both form a complex with Tax and to activate *TBX21* transcription (24, 25). Precipitation with anti-Tax or anti-Sp1 antibodies yielded bands corresponding to both Tax and Sp1, whereas precipitation with the nonspecific IgG antibody as the negative control yielded neither band (Figure 3A), thus demonstrating the existence of a Tax-Sp1 complex in HTLV-1–infected T cells. Second, a ChIP assay using primers encompassing the *TBX21* promoter region (–179 to –59) was performed on the MT-2 cells to confirm the suspected interaction between this Tax-Sp1 complex and the *TBX21* promoter. Precipitation with anti-Tax or anti-Sp1, but not IgG, yielded a PCR product corresponding to the *TBX21* promoter (Figure 3B), which suggests that a Tax-Sp1 complex does bind to the *TBX21* promoter site. Finally, a reporter assay was performed using cells transfected with *TBX21*-Luc, a luciferase reporter plasmid containing the *TBX21* promoter region, to confirm a functional relationship among Tax, Sp1, and *TBX21* transcription. Cotransfection with Sp1 resulted in elevated luciferase activity compared with transfection with the reporter alone, and addition of Tax heightened this effect in a concentration-dependent manner (Figure 3C). These findings suggested that Tax, in concert with Sp1, induces *TBX21* transcription.

HTLV-1–infected Th1-like $CCR4^+$ cells are in the CNS of HAM/TSP patients. We next sought to confirm that HTLV-1–infected $CCR4^+$ T cells infiltrate the spinal cords of HAM/TSP patients and exhibit Th1-like traits, such as T-bet and IFN-γ production. Fluorescent immunohistochemical staining of tissue sections from HAM/TSP patient spinal cord lesions revealed the presence of abundant $CCR4^+$ cells infiltrating around the small blood vessels and coexpressing T-bet and IFN-γ (Figure 4A and Supplemental Figure 4). Further investigation revealed that these $CCR4^+$ cells also expressed CXCR3, the marker for Th1 cells (6). It should be noted that both IFN-γ and CXCR3 expression are reported to be induced by T-bet expression (6). Immunofluorescent staining was also used to demonstrate the existence of HTLV-1–infected $CCR4^+$ cells in the CSF of HAM/TSP patients (Figure 4B). $CCR4^+CXCR3^+$ cells were numerous among cells isolated from the CSF of HAM/TSP patients, representing 73.90% of $CD4^+$ cells isolated from a representative patient (Figure 4C) and 63.63% ± 6.73% of $CD4^+$ cells isolated from all patients ($n = 8$; Figure 4D). However, nearly all of these $CD4^+CCR4^+CXCR3^+$ cells were negative for Ki67, a marker of cell proliferation, in the CSF of the HAM/TSP patients (93.94% ± 2.07%, $n = 3$; Figure 4E). The majority of these $CD4^+CCR4^+CXCR3^+$ cells were also $CD25^+$ (70.16% ± 14.08%, $n = 3$, Supplemental Figure 5), confirming the existence of a substantial $CD4^+CD25^+CCR4^+CXCR3^+$ cell population in the CSF of HAM/TSP patients. Importantly, $CD4^+CCR4^+CXCR3^+$ cells did not make up the majority of PBMCs in HAM/TSP patients nor in HDs; in fact, such cells were very few (HAM/TSP, 3.65% ± 1.96%, $n = 8$; HD, 6.88% ± 3.09%, $n = 4$; Figure 4D). PBMCs were also isolated from ATLL patients for comparison, and $CD4^+CCR4^+CXCR3^-$ cells made up the overwhelming majority (83.03% ± 18.61%, $n = 5$; Supplemental Figure 6).

CCR4 shows potential as a molecular target for HAM/TSP immunotherapy. Analysis of HTLV-1 proviral DNA load in subpopulations of $CD4^+$ PBMCs from HAM/TSP patients confirmed that $CCR4^+$ cells were heavily infected, compared with less than

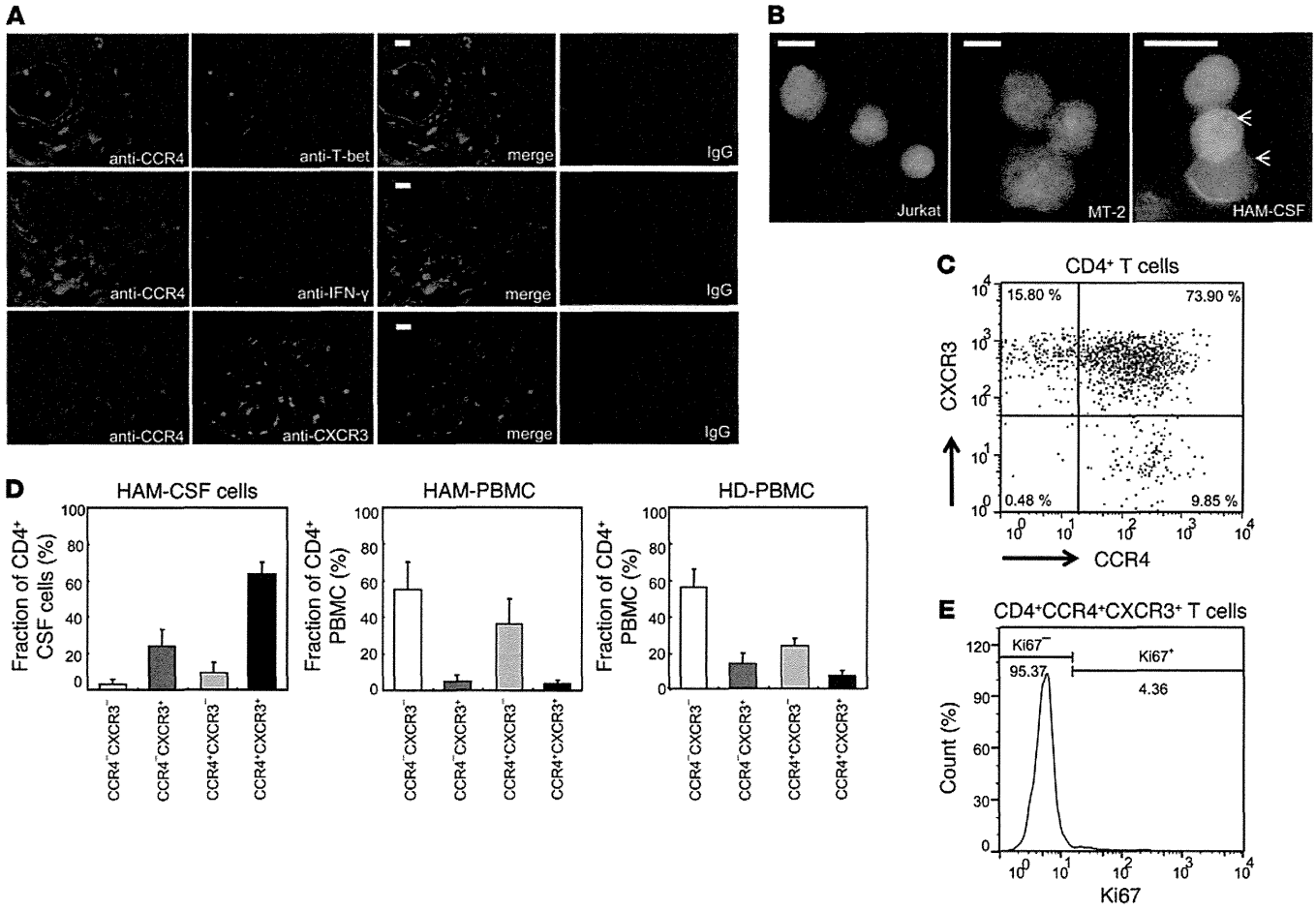

Figure 4. HTLV-1–infected Th1-like CCR4⁺ cells invade the CNS of HAM/TSP patients. (**A**) Detection of CCR4⁺ cells expressing T-bet, IFN-γ, and CXCR3 infiltrating the spinal cord of a HAM/TSP patient. Representative images show immunofluorescent codetection of CCR4 with T-bet, IFN-γ, and CXCR3, as well as the merged images, in thoracic spinal cord sections. Rabbit and goat IgG antibody served as a negative control. Scale bars: 20 μm. (**B**) Presence of HTLV-1–infected CCR4⁺ cells in HAM/TSP patient CSF. Representative images show immunofluorescence-FISH codetection of CCR4 (green) and HTLV-1 provirus (red) in Jurkat cells (uninfected control), MT-2 cells (infected control), and CSF cells from the patients. Arrows denote red provirus signal in the CSF sample. Scale bars: 20 μm. (**C**) CD4⁺ T cells in HAM/TSP patient CSF were mostly CCR4⁺CXCR3⁺. A dot plot of CCR4 and CXCR3 expression in CD4⁺ gated cells isolated from the CSF of a representative HAM/TSP patient is shown. (**D**) CD4⁺CCR4⁺CXCR3⁺ cells were numerous in CSF, but not elevated in peripheral blood, of HAM/TSP patients. Graphs show the percentages of $CCR4^-CXCR3^-$, $CCR4^-CXCR3^+$, $CCR4^+CXCR3^-$ and $CCR4^+CXCR3^+$ T cells among CD4⁺ PBMCs and CSF cells from HAM/TSP patients ($n = 8$) and PBMCs from HDs ($n = 4$). Analysis was performed using FACS. Data are mean ± SD. (**E**) Proliferation was not observed in CD4⁺CCR4⁺CXCR3⁺ cells from HAM/TSP patient CSF. The rate of Ki67 expression, a marker for cell proliferation, is shown for CD4⁺CCR4⁺CXCR3⁺ gated cells from the CSF of a representative HAM/TSP patient.

1% of $CCR4^-$ cells ($n = 7$; Figure 5A). To predict the efficacy of a CCR4⁺ cell–targeting cytotoxic antibody as a treatment for HAM/TSP, PBMCs were isolated from patients ($n = 9$) and analyzed after being cultured with and without the defucosylated chimeric anti-CCR4 monoclonal antibody KM2760 (21) or, for comparison, the steroid therapy prednisolone (PSL). Addition of 1 μg/ml KM2760 significantly reduced the percentage of CCR4⁺ cells, as measured after 7 days ($P = 0.0039$; Figure 5B). As little as 0.1 μg/ml KM2760 was necessary to reduce the HTLV-1 DNA load ($P < 0.05$), whereas PSL had no significant impact (Figure 5C). Use of 1 μg/ml of either KM2760 or PSL was sufficient to suppress spontaneous proliferation of the PBMCs, as measured by ^{3}H-thymidine incorporation ($P < 0.05$ and $P < 0.01$, respectively; Figure 5D) as well as IFN-γ production ($P < 0.05$ and $P < 0.001$, respectively; Figure 5E). Similar results were observed in experiments using cells isolated from the CSF of HAM/TSP patients ($n = 8$): cultures to which 1 μg/ml of KM2760 had been added exhibited reduced HTLV-1 DNA load ($P = 0.0078$; Figure 5F) and IFN-γ production ($P = 0.0391$; Figure 5G). Certain samples shown in Figure 5G did not exhibit this reduction in IFN-γ production; those samples had particularly low cell counts (0.33–2.00 cells/μl), yielding less reliable data. Despite the presence of those lower-quality samples, statistical significance was still established for the sample group as a whole.

Discussion

Previously, we hypothesized that HTLV-1 gives rise to HAM/TSP by altering the behavior of infected cells via Tax expression to yield a new population of Th1-like proinflammatory cells (26). Evidence indicated that a significant portion of this population might be Tregs, as suggested by the CD4⁺CD25⁺CCR4⁺ expres-

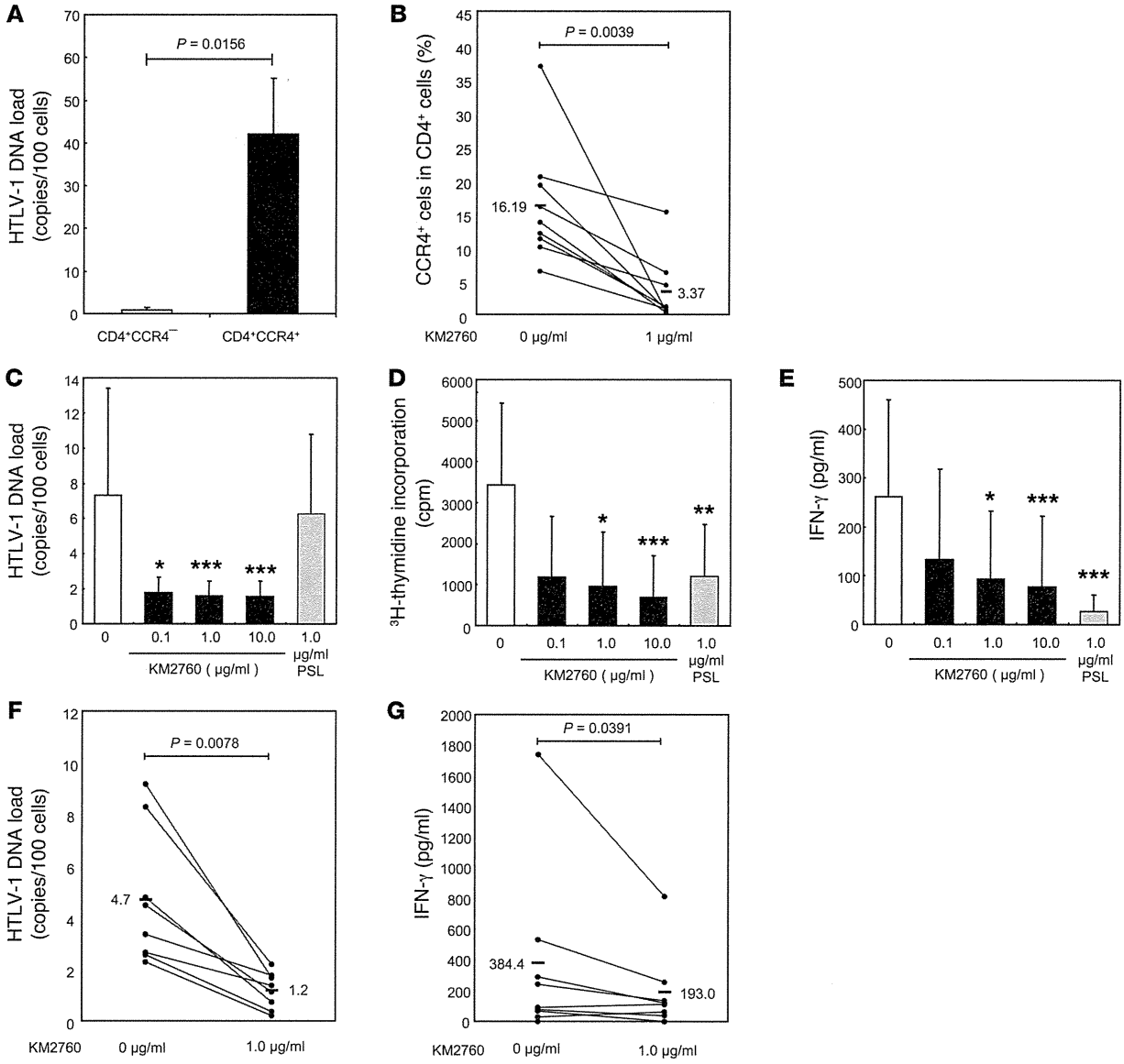

Figure 5. CCR4 shows potential as a molecular target for HAM/TSP immunotherapy. (**A**–**G**) Cells isolated from HAM/TSP patients were sorted via FACS (**A**; $n = 7$) or cultured for 7 days under the following conditions: PBMCs were cultured with various concentrations of KM2760 or 1 μg/ml PSL (**B**–**E**; $n = 9$), and CSF cells were cultured with 1 μg/ml KM2760 (**F** and **G**; $n = 8$). (**A**, **C**, and **F**) HTLV-1 proviral DNA loads were measured using quantitative PCR. (**D**) Degree of spontaneous proliferation was assessed by measuring ^{3}H-thymidine incorporation. (**E** and **G**) IFN-γ production in the culture media was evaluated using CBA assays. HTLV-1 resided in CD4$^+$CCR4$^+$ rather than CCR4$^-$ cells among PBMCs (**A**), and KM2760 treatment effectively targeted these cells (**B**). Consequently, KM2760 treatment successfully reduced HTLV-1 proviral DNA load (**C**), suppressed spontaneous proliferation (**D**), and decreased IFN-γ production (**E**) in PBMC cultures as well as reducing HTLV-1 DNA load (**F**) and IFN-γ production (**G**) in CSF cell cultures derived from HAM/TSP patients. (**A** and **C**–**E**) Data are mean ± SD. (**B**, **F**, and **G**) Thick horizontal bars represent mean value for all patients; line segments represent individual patients. Statistical analyses were performed using Friedman test followed by Dunn test for multiple comparisons (**C**–**E**) or Wilcoxon test (**A**, **B**, **F**, and **G**). $^*P < 0.05$, $^{**}P < 0.01$, $^{***}P < 0.001$ vs. untreated control.

sion profile (19). We suspected that these infected cells may infiltrate the CNS and trigger an inflammatory positive feedback loop, ultimately leading to chronic spinal cord inflammation (27). In the present study, we provided concrete evidence to support these theories on HAM/TSP pathogenesis, with a particular emphasis on the mechanism by which Tax can induce a proinflammatory phenotype intracellularly via transcriptional regulation.

There is strong evidence to support the conclusion that a substantial portion of the Treg population in HAM/TSP patients is infected with HTLV-1 (28, 29). In a previous study, we demonstrated that CD4$^+$CD25$^+$CCR4$^+$ cells were the main reservoir for HTLV-1 in HAM/TSP patients (19), but that expression profile is not exclusive to Tregs. Our present observation that CD4$^+$ T cells positive for FOXP3, a well-established marker for Tregs (10), were more thoroughly infected than the GATA3$^+$ subgroup (Figure 1A) strengthens the argument that Tregs may be the main viral reservoir. It remains debatable whether the virus preferentially infects these cells, promotes their survival (30), or even induces the expression of these

markers. One report postulates that HTLV-1 preferentially infects $CCR4^+$ cells by upregulating CCL22 to encourage cell-to-cell transfer via chemotactic attraction (31). More research is necessary to determine the true mechanism by which infected $CCR4^+$ and $FOXP3^+$ cells become so abundant in HAM/TSP patients.

We demonstrated that the suppressive ability of $CD4^+CD25^+$ $CCR4^+$ cells that characterizes Treg function was impaired by expression of the Tax protein, encoded in the pX region of the HTLV-1 genome (Figure 1B). Prior evidence indicates that Tax may exert these effects via downregulation of FOXP3 expression (20, 32). Transgenic mice expressing Tax exhibit reduced $CD4^+CD25^+FOXP3^+$ Tregs (33) and develop arthritis (34), and transgenic rats expressing HTLV-1 env-pX develop destructive arthropathies, Sjogren syndrome, vasculitis, and polymyositis (35). Collectively, these observations suggest that Tax expression can lead to inflammatory disease by weakening immune tolerance and disrupting homeostasis.

It has long been suspected that in addition to reducing FOXP3 expression, Tax may have the ability to induce IFN-γ production, thereby converting once-suppressive cells into proinflammatory cells. Indeed, intracellular Tax expression has been associated with the rapid upregulation of IFN-γ in infected cells, and researchers have theorized that this upregulation may contribute to the pathogenesis of HTLV-1–associated inflammatory disorders, including HAM/TSP (19, 36, 37). Here we showed at the mRNA level that *Tax* expression stimulated *IFNG* expression; moreover, the effect appeared delayed (Figure 2A), in a manner suggestive of 1 or more intermediate steps in the pathway, rather than direct transcriptional activation. Several candidate pathways have been proposed— such as via NF-κB, STAT1, or STAT5 — but none have been confirmed experimentally (38, 39).

We provided convincing evidence that Tax induces IFN-γ production in infected cells indirectly by amplifying the effects of Sp1 binding to — and increasing the activity of — the *TBX21* promoter: the resulting amplification of T-bet expression was responsible for the rise in IFN-γ production.

T-bet is said to be a Th1-specific T box transcription factor that controls the expression of the hallmark Th1 cytokine, IFN-γ (6). *TBX21*-deficient mice exhibit greater resistance to a variety of inflammatory and autoimmune diseases than their wild-type counterparts (40). Thus, it has been of interest that elevated *TBX21* levels have been found in the PBMCs of HAM/TSP patients (41). We showed that *TBX21* expression was elevated in the $CD4^+CD25^+CCR4^+$ cells of HAM/TSP patients, but not ATLL patients (Figure 2B and Supplemental Figure 1), which suggests that this trait is specific to HAM/TSP pathogenesis. Furthermore, we interpreted the lack of elevation in $CD4^+CD25^-CCR4^-$ cells to indicate that elevated *TBX21* is characteristic of infected cells. Importantly, we clearly demonstrated for the first time that Tax induced T-bet expression (Figure 2, C and E, and Supplemental Figures 2 and 3). Moreover, we showed that this pathway was active in $CD4^+CD25^+CCR4^+$ cells of HAM/TSP patients by silencing Tax expression and observed a corresponding reduction in *TBX21* expression; in the reverse scenario, inducing Tax expression in otherwise-normal $CD4^+CD25^+CCR4^+$ cells from HDs resulted in heightened *TBX21* expression (Figure 2D and Supplemental Figure 2). Finally, we confirmed that this correlation extended to protein production and clearly showed how Tax induces T-bet and subsequently IFN-γ production over time in culture (Figure 2E).

Tax has been reported to stably bind Sp1, a known positive transcriptional regulator of *TBX21* (25, 42). More specifically, interaction with Tax is thought to increase the DNA binding activity of Sp1 (42). Here we used co-IP with samples from the HTLV-1–infected MT-2 cell line to show that endogenous Tax interacted with Sp1 (Figure 3A). Subsequently, ChIP assays revealed that both Sp1 and Tax associated with the *TBX21* promoter region (Figure 3B), a novel finding that supports our theory that Tax and Sp1 together activate *TBX21* transcription. Finally, we showed that in the absence of Sp1, Tax had no significant effect on *TBX21* expression; however, in the presence of Sp1, Tax induced *TBX21* expression in a concentration-dependent manner (Figure 3C). This finding further substantiates our claim that Tax does not directly bind the promoter, but rather acts via Sp1. It should be noted that Tax may induce *TBX21* expression via multiple pathways: it has been reported that Tax enhances STAT1 gene expression in HTLV-1–transformed T cell lines and $CdCl_2$-stimulated JPX-9 cells (38), which suggests that Tax may also induce *TBX21* expression indirectly via STAT1.

The presence of T cell infiltrates in the CNS, indicative of spinal cord inflammation, is a well-known feature of HAM/TSP. Researchers have worked to characterize these cells over the years; together, their findings suggest that the infiltrates are dominated by $CD4^+$ T cells with relatively high proviral loads and elevated Tax and IFN-γ expression (43–45). We hypothesized that a substantial portion of the infiltrate may be made up of infected $CD4^+CCR4^+$ T cells exhibiting Th1-like properties, including IFN-γ production. We used immunohistochemistry to investigate this theory and were able to establish the presence of $CD4^+CCR4^+CXCR3^+$T-$bet^+IFN\text{-}\gamma^+$ cells in spinal cord tissue and HTLV-1–infected $CCR4^+$ cells in the CSF of HAM/TSP patients (Figure 4, A and B). We used FACS analysis to confirm that $CD4^+CCR4^+CXCR3^+$ cells made up the majority of the $CD4^+$ T cells in the HAM/TSP patient CSF (Figure 4C). For the sake of continuity between this and our previous study (19), we also confirmed that the majority of these $CD4^+CCR4^+CXCR3^+$cellswerealso$CD25^+$(SupplementalFigure5), further suggestive of a Treg identity.

We interpret the observation that these $CD4^+CCR4^+CXCR3^+$ cells were virtually nonexistent among PBMCs in HAM/TSP patients (Figure 4D) to mean that the cells had migrated to the CNS, leaving few behind in the periphery. The surprising observation that the Ki67 marker for cell proliferation was negative in the overwhelming majority of $CD4^+CCR4^+CXCR3^+$ cells in the CSF (Figure 4E) signifies that the cells are indeed proliferating elsewhere and subsequently migrating to the CNS. It has in fact been said that HTLV-1–infected cells may be extraordinarily capable of crossing the blood-brain barrier (46). Due to the high proportion of CCR4 positivity among HTLV-1–infected cells (19), the high proviral load in the CSF of HAM/TSP patients (47), and the elevated levels of CCL22 in HAM/TSP patient peripheral blood (30), one might hypothesize that the infected cells migrate across the blood-brain barrier in response to chemokine ligands of CCR4, namely CCL22. However, we found that the CSF of HAM/TSP patients contained only negligible amounts of CCL22, instead favoring the CXCR3 ligand CXCL10 (48). We now postulate that

$CD4^+CCR4^+CXCR3^+$ T cells and other $CXCR3^+$ cells may migrate to the CNS via chemotaxis induced by CXCL10 secreted by astrocytes in the CNS. Previously, we showed that these astrocytes produce CXCL10 in response to IFN-γ, and these levels are further amplified by the invading $CXCR3^+$ cells (27). Together, these findings indicate that a positive feedback loop involving the recruitment of proinflammatory cells to the CNS is the source of chronic inflammation in HAM/TSP, and that the original trigger is the migration of IFN-γ–producing HTLV-1–infected cells to the CNS. Where these proinflammatory cells are primarily proliferating, and why they proliferate at different rates in different settings, are questions to be addressed in future studies.

Our findings in this and previous studies imply that targeting $CCR4^+$ cells could constitute an effective treatment for HAM/TSP. Indeed, this strategy is already in play for ATLL patients, the majority of whom suffer from $CCR4^+$ T cell–derived cancers (7). The humanized defucosylated anti-CCR4 monoclonal antibody KW-0761, which has been shown to induce CCR4-specific ADCC, has been approved as a treatment for ATLL (49, 50). The observation that the majority of infected $CD4^+$ PBMCs in HAM/TSP patients were $CCR4^+$ (Figure 5A) suggests that an anti-CCR4 antibody with ADCC properties might be used to effectively treat HAM/TSP patients as well. Steroids are currently the standard of care for HAM/TSP patients, but this approach is not considered optimal: as with many nonspecific treatments, the effectiveness is limited, and the side effects are numerous (51). Here we compared the effects of the defucosylated chimeric anti-CCR4 monoclonal antibody KM2760 (21) with those of the steroid PSL on ex vivo cultures of cells from HAM/TSP patients. Although PSL had more potent effects per microgram, both treatments successfully reduced cell proliferation and IFN-γ production (Figure 5, D, E, and G). In addition, even a small dose of the antibody effectively reduced proviral load, whereas PSL treatment had no significant effect (Figure 5, C and F). These findings support the main premise of this paper, namely, that $CCR4^+$ cells are major viral reservoirs and producers of IFN-γ. Our study is the first to test the effects of such an antibody-based treatment on cells from HAM/TSP patients; the results were promising, and a clinical trial investigating the in vivo effectiveness in HAM/TSP patients is now underway. Importantly, our research indicates that even if the antibody does not cross the blood-brain barrier, it could be therapeutically effective against spinal cord inflammation by eliminating the proinflammatory $CCR4^+$ cells in the peripheral blood that would have migrated to the CNS.

Until very recently, there had been no reports of T cell character changing from suppressive to inflammatory in response to internal transcriptional alterations induced intracellularly by viral products. There have been many reports of Tregs transforming in the presence of inflammation due to the influence of cytokines, including instances where FOXP3 expression is lost and even cases where IFN-γ production is gained (12, 13). The only report of a similar phenomenon occurring via an intracellular virus-induced pathway states that the HTLV-1 basic leucine zipper (HBZ) gene product can reduce the expression of FOXP3 in HBZ-transgenic mouse Tregs (52). Here we showed for the first time that the HTLV-1 virus can similarly affect gene expression in human cells, inducing IFN-γ production, as well as reduce suppressive function. Collectively, the research to date suggests that HTLV-1 may preferentially infect $CCR4^+$ cells, including Tregs, and induce transcriptional changes via Tax that not only reduce FOXP3 expression, but also induce T-bet expression and consequently IFN-γ production, yielding a proinflammatory immune imbalance. While there is considerable evidence to support this theory, further experiments are necessary to prove that this pathway is indeed the origin of HAM/TSP chronic inflammation. However, here we have directly shown that the HTLV-1 protein product Tax can induce the expression of the Th1 master transcription factor T-bet, which certainly implies that HTLV-1 is capable of activating inherent plasticity in T cells and shifting their gene expression profiles toward a Th1-like state.

Methods

Patient selection and sample preparation. The study included HTLV-1–noninfected HDs ($n = 8$, 4 male and 4 female; mean age, 36 yr), asymptomatic carriers ($n = 6$, 4 male and 2 female; mean age, 56 yr), ATLL patients ($n = 6$, 2 male and 4 female; mean age, 68 yr), and HAM/TSP patients ($n = 31$, 9 male and 22 female; mean age, 61 yr). Diagnosis of ATLL was based on the criteria established by Shimoyama (53). HTLV-1 seropositivity was determined by a particle agglutination assay (Serodia-HTLV-1) and confirmed by Western blot (SRL Inc.). HAM/TSP was diagnosed according to WHO guidelines (54).

Samples of PBMCs were prepared using density gradient centrifugation (Pancoll; PAN-Biotech) and viably cryopreserved in liquid nitrogen (Cell Banker 1; Mitsubishi Chemical Medience Corp.). CSF samples were taken from 17 HAM/TSP patients. CSF cells were isolated by centrifugation and cryopreserved in the aforementioned freezing medium until use. Thoracic spinal cord tissue samples from 1 HAM/TSP patient were obtained postmortem, fixed in 10% formalin, and embedded in paraffin.

Antibodies. For FACS studies, labeled anti-CD3 (UCHT1), anti-CD4 (OKT4), anti-GATA3 (TWAJ), and anti-FOXP3 (PCH101) were purchased from eBioscience, and labeled anti-CCR4 (1G1), anti-CD25 (BC96), anti-CXCR3 (1C6), anti–T-bet (4B10), and anti-Ki67 (B56) were purchased from BD Biosciences. For IP studies, anti-Sp1 (PEP2) and normal IgG were purchased from Santa Cruz Biotechnology Inc., and anti-Tax (Lt-4) was prepared as described previously (55). For immunofluorescence studies, anti-CCR4, anti–IFN-γ, and anti-CXCR3 were purchased from Abcam; anti–T-bet was purchased from Santa Cruz Biotechnology Inc.; and Alexa Fluor 488– and Alexa Fluor 594–conjugated secondary antibodies were purchased from Invitrogen. Kyowa Hakko Kirin Co. Ltd. provided KM2760, a chimeric anti-CCR4 IgG1 monoclonal antibody (21).

Plasmids. The *TBX21*-Luc reporter gene plasmid was constructed as described previously (25). The 100-bp promoter fragment (–101 to –1) in the 5′-flanking region of the human *TBX21* gene was obtained by PCR using human PBMC genomic DNA as the template. Primers used for PCR were 5′-CGCCTCGAGGGCGGGGTGGGGCGAGGCGG-3′ and 5′-CCCAAGCTTCTGTCACTAGAGTCGCAGCGCTTT-3′. The amplified PCR product was digested with XhoI/HindIII and cloned into pPicaGene-Basic vector II (Toyo-ink), which yielded *TBX21*-Luc. Creation of the human Sp1 construct with HA-tag added to the N terminus was accomplished via real-time RT-PCR amplification of human PBMC cDNA with the following primers: Sp1 forward, 5′-CGCGAATTCATGAGCGACCAAGATCACTCCATGGA-3′; Sp1 reverse, 5′-CGCCTCGAGTCAGAAGCCATTGCCACTGATATTAATGGAC-3′. The amplified fragment was digested with EcoRI/XhoI and

subcloned into HA-tagged pcDNA3 (Invitrogen). Tax construct with FLAG-tag added to the N terminus was prepared via PCR amplification of template DNA (56) with the following primers: Tax forward, 5′-CGCGAATTCATGGCCCACTTCCCAGGGTTT-3′; Tax reverse, 5′-CGCCTCGAGTCAGACTTCTGTTTCACGGAAATGTTTTTC-3′. The amplified fragment was digested with EcoRI/XhoI and subcloned into FLAG-tagged pcDNA3. The plasmid HTLV-1 provirus (pUC/HTLV-1) was provided by T. Watanabe (University of Tokyo, Tokyo, Japan) (57). A lentiviral vector, CSIICMV, was used as a null expression vector for lentiviral infection (provided by H. Miyoshi, RIKEN BioResource Center, Tsukuba, Japan) (58). CSIICMV/GFP and CSIICMV/GFP-Tax, which express GFP and GFP fused Tax, were constructed by inserting digested GFP and GFP-Tax from pEGFP (Clontech) and pEGFP-Tax, respectively, into CSIICMV.

Flow cytometric analysis. PBMCs and CSF cells were immunostained with various combinations of the following fluorescence-conjugated antibodies that tag cell surface markers: CD3 (UCHT1), CD4 (OKT4), CD25 (BC96), CCR4 (1G1), CXCR3 (1C6). In some experiments, cells were fixed with a staining buffer set (eBioscience), then intracellularly stained with antibodies against T-bet (4B10), FOXP3 (PCH101), and GATA3 (TWAJ). Cells were stained with a saturating concentration of antibody in the dark (4°C, 30 minutes) and washed twice before analysis using FACSCalibur or LSR II (BD Biosciences). Data were processed using FlowJo software (TreeStar). For cell sorting, JSAN (Bay Bioscience) was used, and the purity exceeded 95%.

Cell isolation. $CD4^+CD25^+CCR4^+$ cells, $CD4^+CD25^-CCR4^-$ cells, $CD4^+GATA3^+$ cells, and $CD4^+FOXP3^+$ cells were separated by FACS sorting. $CD4^+$ T cells were isolated from PBMCs using negative selection with magnetic beads (MACS $CD4^+$ T cell isolation kit; Miltenyi Biotec). $CD4^+CCR4^-$ or $CD4^+CCR4^+$ cells were then isolated from these $CD4^+$ T cells using positive selection with anti-CCR4 Ab (1G1) and rat anti-mouse IgG1 microbeads (Miltenyi Biotec).

Cell culture conditions. HEK293 cells were cultured in MEM (Wako Pure Chemical Industries) supplemented with 10% heat-inactivated FBS (Gibco, Invitrogen) and 1% penicillin/streptomycin (P/S) (Wako Pure Chemical Industries). HEK293T cells were cultured in DMEM–high glucose (Sigma-Aldrich) supplemented with 10% FBS and 1% P/S. Jurkat, MT-2, and JPX-9 cells were cultured in RPMI 1640 medium (Wako Pure Chemical Industries) supplemented with 10% FBS and 1% P/S. JPX-9 is a subline of Jurkat carrying Tax under the control of the metallothionein promoter (provided by M. Nakamura, Tokyo Medical and Dental University, Tokyo, Japan) (59), by which Tax expression is inducible by the addition of 20 μM $CdCl_2$ (Nacalai Tesque Inc.). PBMCs, $CD4^+CCR4^+$ cells, $CD4^+CD25^+CCR4^+$ cells, and $CD4^+CD25^-CCR4^-$ cells isolated from HDs or HAM/TSP patients were cultured in RPMI 1640 medium supplemented with 5% human AB serum (Gibco, Invitrogen) and 1% P/S.

Gene expression profiling and analyses. For transcriptional profiling, $CD4^+CD25^+CCR4^+$ T cells from a HAM/TSP patient, an ATLL patient, and an HD were separated using FACS sorting. Total RNA was prepared using ISOGEN (Nippon gene) following the manufacturer's recommendations. RNA was amplified and labeled with cyanine 3 (Cy3) using an Agilent Quick Amp Labeling Kit, 1-color (Agilent Technologies), following the manufacturer's instructions. For each hybridization, Cy3-labeled cRNA were fragmented and hybridized to an Agilent Human GE 4x44K Microarray (design ID 014850). After washing, microarrays were scanned using an Agilent DNA microarray scanner. Intensity values of each scanned feature were quantified using Agilent feature extraction software (version 9.5.3.1), which performs background subtractions. All data were analyzed using GeneSpring GX software (Agilent Technologies). There were a total of 41,000 probes on Agilent Human GE 4x44K Microarray (design ID 014850), not including control probes. Microarray data were deposited in GEO (accession no. GSE57259).

Real-time PCR and real-time RT-PCR. The HTLV-1 proviral DNA load was measured using ABI Prism 7500 SDS (Applied Biosystems) as described previously (19). For real-time RT-PCR analysis, total RNA isolation and cDNA synthesis were performed as described previously (19). Real-time PCR reactions were carried out using TaqMan Universal Master Mix (Applied Biosystems) and Universal Probe Library assays designed using ProbeFinder software (Roche Applied Science). ABI Prism 7500 SDS was programmed to have an initial step of 2 minutes at 50°C and 10 minutes at 95°C, followed by 45 cycles of 15 seconds at 95°C and 1 minute at 60°C. The primers used were as follows: *TBX21*, 5′-TGTGGTCCAAGTTTAATCAGCA-3′ (forward) and 5′-TGACAGGAATGGGAACATCC-3′ (reverse) (probe no. 9; Roche Applied Science); *Tax*, 5′-ATACAACCCCCAACATTCCA-3′ (forward) and 5′-TTTCGGAAGGGGGAGTATTT-3′ (reverse) (probe no. 69; Roche Applied Science). The primers and probes for detecting *Tax*, *IFNG*, and *GAPDH* mRNA were described previously (19). Relative quantification of mRNA was performed using the comparative Ct method using GAPDH as an endogenous control. For each sample, target gene expression was normalized to the expression of GAPDH, calculated as $2^{-(Ct[target]-Ct[GAPDH])}$.

Virus preparation and cell infection. 293T cells (1×10^6) plated in 100-mm dishes were cotransfected with the appropriate lentiviral-GFP or lentiviral-GFP-Tax expression vector (17 μg), vesicular stomatitis virus G expression vector VSV-G (pMD.G) (5 μg), rev expression vector pRSVRev (5 μg), and gag-pol expression vector pMDLg/pRRE (12 μg) (60) using Lipofectamine 2000 (Invitrogen) according to the manufacturer's protocol. After 4 hours, cells were washed 3 times with PBS, 5 ml of new medium was added, and cells were incubated for 48 hours. Culture supernatants were harvested and filtered through 0.45-μm pore size filters. Lentivirus was concentrated approximately 40-fold by low centrifugation at 6,000 *g* for 16 hours and resuspended in 2 ml RPMI 1640 medium. Freshly isolated $CD4^+CD25^+CCR4^+$ T cells were activated using Treg Suppression Inspector (Anti-Biotin MACSiBead Particles preloaded with biotinylated CD2, CD3, and CD28 antibodies) according to the manufacturer's protocol (Miltenyi Biotec). After being cultured for 36 hours, cells were transduced with equal amounts of the GFP or GFP-Tax lentivirus (MOI 15), followed by centrifugation for 1 hour at 780 *g*, 32°C. After being cultured for 4 hours at 32°C, cells were washed with culture medium and cultured in round-bottomed 96-well plates at 37°C.

Treg suppression assay. A study was conducted to compare the capacities of GFP versus GFP-Tax lentivirus–infected $CD4^+CD25^+CCR4^+$ T cells to suppress cell proliferation. T cell samples were taken from HDs, and 5×10^4 $CD4^+CD25^-$ T cells were stimulated with the Treg Suppression Inspector (see above) according to the manufacturer's instructions. These cells were then cocultured with 5×10^4 GFP lentivirus–infected $CD4^+CD25^+CCR4^+$ T cells or GFP-Tax lentivirus–infected $CD4^+CD25^+CCR4^+$ T cells. After culturing for 4 days, cell proliferation was measured using a ^{3}H-thymidine incorporation assay as described previously (19).

RNA interference assay. siRNA was synthesized chemically at Hokkaido System Science. The sequences of siRNA oligonucleotides were as follows: Tax, 5′-GGCCUUAUUUGGACAUUUATT-3′ and 5′-UAAAUGUCCAAAUAAGGCCTT-3′ (31); Luc, 5′-CGUACGCG-GAAUACUUCGATT-3′ and 5′-UCGAAGUAUUCCGCGUACGTT3′. Next, 100 pmol annealed RNA duplex was transfected using Human T cell Amaxa Nucleofector Kit according to the manufacturer's recommendations (Lonza). 100 pmol Luc siRNA was used as a negative control. Cells were incubated for 48 hours and then harvested and subjected to real-time RT-PCR analysis.

Measurement of IFN-γ. IFN-γ concentration in the culture supernatant was measured with a cytometric bead array kit (BD Biosciences) using a FACSCalibur flow cytometer (BD Biosciences) according to the manufacturer's instructions.

IP. Approximately 1 mg of MT-2 nuclear extracts were incubated with 5 μg anti-Tax, anti-Sp1, or normal IgG coupled with protein G–agarose (Roche Applied Science) in IP buffer (10 mM HEPES [pH 7.9], 100 mM KCl, 1 mM EDTA, 1 mM dithiothreitol, 0.1% NP-40, 1 mM Na_3VO_4, 5 mM NaF, 2 μg/ml aprotinin, 2 μg/ml leupeptin, and 2 μg/ml pepstatin) for 2 hours. The precipitated proteins were washed with the IP buffer, separated by 10% SDS-PAGE, and immunoblotted with anti-Tax or anti-Sp1 antibodies.

ChIP assay. ChIP assay was performed using a ChIP assay kit (Upstate Biotechnology) with some modifications. Briefly, 5×10^6 MT-2 cells were fixed with 1% formaldehyde at 37°C for 25 minutes and washed twice with PBS. Cells were subsequently harvested and sonicated in lysis buffer. Precleared chromatin samples were immunoprecipitated with 5 μg anti-Tax antibody, anti-Sp1 antibody, or normal IgG for 16 hours at 4°C. Immune complexes were collected with salmon sperm DNA/protein G–sepharose for 90 minutes with rotation, washed, and then incubated at 65°C for 6 hours for reverse cross-linking. Chromatin DNA was extracted and analyzed using PCR with primers for the *TBX21* promoter region (–179 to –59; forward, 5′-GCCAAGAGCGTAGAATTTGC-3′; reverse, 5′-CGCTTT-GCTGTGGCTTTATG-3′) (25, 61). Amplification was performed using ExTaq (Takara Bio) with 1 cycle at 95°C for 5 minutes followed by 30 cycles of 95°C for 30 seconds, 54°C for 30 seconds, and 72°C for 30 seconds. Amplified products were analyzed using 8% polyacrylamide gel electrophoresis.

Luciferase assay. For transient transfection, HEK293 cells were seeded at 5×10^4 cells/well into 24-well plates. After 12 hours, medium was changed to MEM supplemented with 10% FBS and 1% P/S, and each plasmid was transfected with CellPhect Transfection Kit according to the manufacturer's recommendations (GE Healthcare). 50 ng pRSV-βgal plasmid was included in each transfection experiment to control for the efficiency of transfection. The total amount of transfected DNA was kept constant with pcDNA3 in all samples. After 48 hours, cells were lysed with Passive Lysis Buffer (Promega), and luciferase activity was measured using the Promega luciferase assay system and MicroLumat Plus LB96V (Berthold Technologies). Values were normalized to β-galactosidase activity as an internal control.

Tissue staining. Formalin-fixed thoracic spinal cord tissue sections were deparaffinized in xylene and rehydrated in a series of graded alcohols and distilled water. The antigenicity of the tissue sections was recovered using a standard microwave heating technique. For immunofluorescence, the slides were incubated in PBS with 10% goat serum for 1 hour at room temperature, then in anti-CCR4 antibody, anti–T-bet antibody, anti–IFN-γ antibody, and anti-CXCR3 antibody overnight at 4°C, labeled with Alexa Fluor 488– or Alexa Fluor 594–conjugated secondary antibody, and examined under a fluorescence microscope (Nikon eclipse E600 with fluorescence filter Nikon F-FL; Nikon Instech) with rabbit or goat IgG as the negative control. Tissue sections were also stained with H&E.

Immunofluorescence staining and immunofluorescence-FISH. Jurkat cells, MT-2 cells, and cells from the CSF of 3 HAM/TSP patients were attached to slides using a cytospin centrifuge (Thermo Fisher Scientific) and fixed in 4% paraformaldehyde (Wako Pure Chemical Industries) for 30 minutes. The slides were washed with PBS and then pretreated as follows: slides were immersed in room temperature 0.2M HCl for 20 minutes, followed by 0.2% Triton-X/PBS for 10 minutes, and finally 0.005% pepsin/0.1M HCl heated to 37°C for 5 minutes. After pretreatment, the slides were stained using the immunofluorescence Can Get Signal kit (TOYOBO) according the manufacturer's instructions with anti-CCR4 as the primary antibody and Alexa Fluor 488–conjugated anti-goat IgG as the secondary antibody. After again being fixed with 4% paraformaldehyde, cells were incubated with a nick-translated (Spectrum Red) pUC/HTLV-1 DNA probe, first for 5 minutes at 70°C and then overnight at 37°C. Images were obtained under an automated research microscope (Leica DMRA2) and analyzed with CW4000 FISH software (Leica Microsystems).

Proliferation assay. PBMCs from HAM/TSP patients were plated into 96-well round-bottomed plates (1×10^5 cells/well) and cultured without any mitogenic stimuli. Cell proliferation was measured using a ^{3}H-thymidine incorporation assay as described previously (19).

Statistics. Paired 2-tailed Student's *t* test and Wilcoxon test were used for within-group comparisons. Unpaired 2-tailed Student's *t* test or Mann-Whitney *U* test was used for between-group comparisons. 1-way ANOVA was used for multiple comparisons, followed by Dunnett or Tukey test. Friedman test was used for paired multiple comparisons, followed by Dunn test. Statistical analyses were performed using Graphpad Prism 5 (GraphPad Software Inc.). A *P* value less than 0.05 was considered significant.

Study approval. Written informed consent was obtained from all patients before the study, which was reviewed and approved by the Institutional Ethics Committee at St. Marianna University and conducted in compliance with the tenets of the Declaration of Helsinki.

Acknowledgments

The authors acknowledge the excellent technical assistance provided by Yumiko Hasegawa, M. Koike, Y. Suzuki-Ishikura, and Y. Saito. This work was partly supported by project "Research on Measures for Intractable Disease"; by a matching fund subsidy from the Ministry of Health Labour and Welfare; by JSPS KAKENHI grant nos. 24790898, 25461294, and 25461293; by the Takeda Science Foundation; and by the Daiichi Sankyo Foundation of Life Science.

Address correspondence to: Yoshihisa Yamano, Department of Rare Diseases Research, Institute of Medical Science, St. Marianna University School of Medicine, 2-16-1 Sugao, Miyamae-ku, Kanagawa 216-8512, Japan. Phone: 81.44.977.8111; E-mail: yyamano@marianna-u.ac.jp.

1. Murphy KM, Stockinger B. Effector T cell plasticity: flexibility in the face of changing circumstances. *Nat Immunol*. 2010;11(8):674–680.
2. Cosmi L, Maggi L, Santarlasci V, Liotta F, Annunziato F. T helper cells plasticity in inflammation. *Cytometry A*. 2014;85(1):36–42.
3. Long SA, Buckner JH. CD4+FOXP3+ T regulatory cells in human autoimmunity: more than a numbers game. *J Immunol*. 2011;187(5):2061–2066.
4. Zhou X, Bailey-Bucktrout S, Jeker LT, Bluestone JA. Plasticity of CD4(+) FoxP3(+) T cells. *Curr Opin Immunol*. 2009;21(3):281–285.
5. Hori S, Nomura T, Sakaguchi S. Control of regulatory T cell development by the transcription factor Foxp3. *Science*. 2003;299(5609):1057–1061.
6. Zhu J, Paul WE. CD4 T cells: fates, functions, and faults. *Blood*. 2008;112(5):1557–1569.
7. Ishida T, Ueda R. Immunopathogenesis of lymphoma: focus on CCR4. *Cancer Sci*. 2011;102(1):44–50.
8. Finney OC, Riley EM, Walther M. Phenotypic analysis of human peripheral blood regulatory T cells (CD4+FOXP3+CD127lo/–) ex vivo and after in vitro restimulation with malaria antigens. *Eur J Immunol*. 2010;40(1):47–60.
9. Mjosberg J, Berg G, Jenmalm MC, Ernerudh J. FOXP3+ regulatory T cells and T helper 1, T helper 2, and T helper 17 cells in human early pregnancy decidua. *Biol Reprod*. 2010;82(4):698–705.
10. Williams LM, Rudensky AY. Maintenance of the Foxp3-dependent developmental program in mature regulatory T cells requires continued expression of Foxp3. *Nat Immunol*. 2007;8(3):277–284.
11. Bennett CL, et al. The immune dysregulation, polyendocrinopathy, enteropathy, X-linked syndrome (IPEX) is caused by mutations of FOXP3. *Nat Genet*. 2001;27(1):20–21.
12. Gao Y, et al. Molecular mechanisms underlying the regulation and functional plasticity of FOXP3(+) regulatory T cells. *Genes Immun*. 2012;13(1):1–13.
13. Dominguez-Villar M, Baecher-Allan CM, Hafler DA. Identification of T helper type 1-like, Foxp3+ regulatory T cells in human autoimmune disease. *Nat Med*. 2011;17(6):673–675.
14. Sakaguchi S, et al. Foxp3+ CD25+ CD4+ natural regulatory T cells in dominant self-tolerance and autoimmune disease. *Immunol Rev*. 2006;212:8–27.
15. Viglietta V, Baecher-Allan C, Weiner HL, Hafler DA. Loss of functional suppression by CD4+CD25+ regulatory T cells in patients with multiple sclerosis. *J Exp Med*. 2004;199(7):971–979.
16. Kanangat S, et al. Disease in the scurfy (sf) mouse is associated with overexpression of cytokine genes. *Eur J Immunol*. 1996;26(1):161–165.
17. Lyon MF, Peters J, Glenister PH, Ball S, Wright E. The scurfy mouse mutant has previously unrecognized hematological abnormalities and resembles Wiskott-Aldrich syndrome. *Proc Natl Acad Sci U S A*. 1990;87(7):2433–2437.
18. Clark LB, Appleby MW, Brunkow ME, Wilkinson JE, Ziegler SF, Ramsdell F. Cellular and molecular characterization of the scurfy mouse mutant. *J Immunol*. 1999;162(5):2546–2554.
19. Yamano Y, et al. Abnormally high levels of virus-infected IFN-γ+ CCR4+ CD4+ CD25+ T cells in a retrovirus-associated neuroinflammatory disorder. *PLoS One*. 2009;4(8):e6517.
20. Yamano Y, et al. Virus-induced dysfunction of CD4+CD25+ T cells in patients with HTLV-I-associated neuroimmunological disease. *J Clin Invest*. 2005;115(5):1361–1368.
21. Niwa R, et al. Defucosylated chimeric anti-CC chemokine receptor 4 IgG1 with enhanced antibody-dependent cellular cytotoxicity shows potent therapeutic activity to T-cell leukemia and lymphoma. *Cancer Res*. 2004;64(6):2127–2133.
22. Yoshida M, Seiki M, Yamaguchi K, Takatsuki K. Monoclonal integration of human T-cell leukemia provirus in all primary tumors of adult T-cell leukemia suggests causative role of human T-cell leukemia virus in the disease. *Proc Natl Acad Sci U S A*. 1984;81(8):2534–2537.
23. Cook LB, Rowan AG, Melamed A, Taylor GP, Bangham CR. HTLV-1-infected T cells contain a single integrated provirus in natural infection. *Blood*. 2012;120(17):3488–3490.
24. Zhang L, Zhi H, Liu M, Kuo YL, Giam CZ. Induction of p21(CIP1/WAF1) expression by human T-lymphotropic virus type 1 Tax requires transcriptional activation and mRNA stabilization. *Retrovirology*. 2009;6:35.
25. Yu J, et al. Transcriptional control of human T-BET expression: the role of Sp1. *Eur J Immunol*. 2007;37(9):2549–2561.
26. Araya N, et al. Human T-lymphotropic virus type 1 (HTLV-1) and regulatory T cells in HTLV-1-associated neuroinflammatory disease. *Viruses*. 2011;3(9):1532–1548.
27. Ando H, et al. Positive feedback loop via astrocytes causes chronic inflammation in virus-associated myelopathy. *Brain*. 2013; 136(pt 9):2876–2887.
28. Kohno T, et al. Possible origin of adult T-cell leukemia/lymphoma cells from human T lymphotropic virus type-1-infected regulatory T cells. *Cancer Sci*. 2005;96(8):527–533.
29. Satou Y, Utsunomiya A, Tanabe J, Nakagawa M, Nosaka K, Matsuoka M. HTLV-1 modulates the frequency and phenotype of FoxP3+CD4+ T cells in virus-infected individuals. *Retrovirology*. 2012;9:46.
30. Toulza F, et al. Human T-lymphotropic virus type 1-induced CC chemokine ligand 22 maintains a high frequency of functional FoxP3+ regulatory T cells. *J Immunol*. 2010;185(1):183–189.
31. Hieshima K, Nagakubo D, Nakayama T, Shirakawa AK, Jin Z, Yoshie O. Tax-inducible production of CC chemokine ligand 22 by human T cell leukemia virus type 1 (HTLV-1)-infected T cells promotes preferential transmission of HTLV-1 to CCR4-expressing CD4+ T cells. *J Immunol*. 2008;180(2):931–939.
32. Grant C, Oh U, Yao K, Yamano Y, Jacobson S. Dysregulation of TGF-β signaling and regulatory and effector T-cell function in virus-induced neuroinflammatory disease. *Blood*. 2008;111(12):5601–5609.
33. Ohsugi T, Kumasaka T. Low CD4/CD8 T-cell ratio associated with inflammatory arthropathy in human T-cell leukemia virus type I Tax transgenic mice. *PLoS One*. 2011;6(4):e18518.
34. Iwakura Y, et al. Induction of inflammatory arthropathy resembling rheumatoid arthritis in mice transgenic for HTLV-I. *Science*. 1991;253(5023):1026–1028.
35. Nakamaru Y, et al. Immunological hyperresponsiveness in HTLV-I LTR-env-pX transgenic rats: a prototype animal model for collagen vascular and HTLV-I-related inflammatory diseases. *Pathobiology*. 2001;69(1):11–18.
36. Hanon E, et al. High production of interferon gamma but not interleukin-2 by human T-lymphotropic virus type I-infected peripheral blood mononuclear cells. *Blood*. 2001;98(3):721–726.
37. Yamazato Y, Miyazato A, Kawakami K, Yara S, Kaneshima H, Saito A. High expression of p40(tax) and pro-inflammatory cytokines and chemokines in the lungs of human T-lymphotropic virus type 1-related bronchopulmonary disorders. *Chest*. 2003;124(6):2283–2292.
38. Nakamura N, et al. Human T-cell leukemia virus type 1 Tax protein induces the expression of STAT1 and STAT5 genes in T-cells. *Oncogene*. 1999;18(17):2667–2675.
39. Sun SC, Yamaoka S. Activation of NF-kappaB by HTLV-I and implications for cell transformation. *Oncogene*. 2005;24(39):5952–5964.
40. Lazarevic V, Glimcher LH. T-bet in disease. *Nat Immunol*. 2011;12(7):597–606.
41. Nishiura Y, Nakamura T, Fukushima N, Moriuchi R, Katamine S, Eguchi K. Increased mRNA expression of Th1-cytokine signaling molecules in patients with HTLV-I-associated myelopathy/tropical spastic paraparesis. *Tohoku J Exp Med*. 2004;204(4):289–298.
42. Trejo SR, Fahl WE, Ratner L. The tax protein of human T-cell leukemia virus type 1 mediates the transactivation of the c-sis/platelet-derived growth factor-B promoter through interactions with the zinc finger transcription factors Sp1 and NGFI-A/Egr-1. *J Biol Chem*. 1997;272(43):27411–27421.
43. Furuya T, et al. Heightened transmigrating activity of CD4-positive T cells through reconstituted basement membrane in patients with human T-lymphotropic virus type I-associated myelopathy. *Proc Assoc Am Physicians*. 1997; 109(3):228–236.
44. Moritoyo T, et al. Detection of human T-lymphotropic virus type I p40tax protein in cerebrospinal fluid cells from patients with human T-lymphotropic virus type I-associated myelopathy/tropical spastic paraparesis. *J Neurovirol*. 1999;5(3):241–248.
45. Umehara F, Izumo S, Ronquillo AT, Matsumuro K, Sato E, Osame M. Cytokine expression in the spinal cord lesions in HTLV-I-associated myelopathy. *J Neuropathol Exp Neurol*. 1994;53(1):72–77.
46. Matsuura E, Yamano Y, Jacobson S. Neuroimmunity of HTLV-I Infection. *J Neuroimmune Pharmacol*. 2010;5(3):310–325.
47. Nagai M, Yamano Y, Brennan MB, Mora CA, Jacobson S. Increased HTLV-I proviral load and preferential expansion of HTLV-I Tax-specific CD8+ T cells in cerebrospinal fluid from patients with HAM/TSP. *Ann Neurol*. 2001;50(6):807–812.
48. Sato T, et al. CSF CXCL10, CXCL9, and neopterin as candidate prognostic biomarkers for HTLV-1-associated myelopathy/tropical spastic paraparesis. *PLoS Negl Trop Dis*. 2013;7(10):e2479.
49. Yamamoto K, et al. Phase I study of KW-0761, a defucosylated humanized anti-CCR4 antibody, in relapsed patients with adult T-cell leukemia-lymphoma and peripheral T-cell lymphoma.

J Clin Oncol. 2010;28(9):1591–1598.
50. Ishida T, et al. Defucosylated anti-CCR4 monoclonal antibody (KW-0761) for relapsed adult T-cell leukemia-lymphoma: a multicenter phase II study. *J Clin Oncol*. 2012;30(8):837–842.
51. Yamano Y, Sato T. Clinical pathophysiology of human T-lymphotropic virus-type 1-associated myelopathy/tropical spastic paraparesis. *Front Microbiol*. 2012;3:389.
52. Yamamoto-Taguchi N, et al. HTLV-1 bZIP factor induces inflammation through labile Foxp3 expression. *PLoS Pathog*. 2013;9(9):e1003630.
53. Shimoyama M. Diagnostic criteria and classification of clinical subtypes of adult T-cell leukaemia-lymphoma. A report from the Lymphoma Study Group (1984–1987). *Br J Haematol*. 1991;79(3):428–437.
54. Osame M. Review of WHO Kagoshima meeting and diagnostic guidelines for HAM/TSP. In: Blattner W, ed. *Human Retrovirology: HTLV*. New York, New York, USA: Raven Press; 1990:191–197.
55. Tanaka Y, et al. An antigenic structure of the trans-activator protein encoded by human T-cell leukemia virus type-I (HTLV-I), as defined by a panel of monoclonal antibodies. *AIDS Res Hum Retroviruses*. 1992;8(2):227–235.
56. Yoshiki T, et al. Models of HTLV-I-induced diseases. Infectious transmission of HTLV-I in inbred rats and HTVL-I env-pX transgenic rats. *Leukemia*. 1997;11(suppl 3):245–246.
57. Kamihira S, et al. Intra- and inter-laboratory variability in human T-cell leukemia virus type-1 proviral load quantification using real-time polymerase chain reaction assays: a multi-center study. *Cancer Sci*. 2010;101(11):2361–2367.
58. Bai Y, et al. Effective transduction and stable transgene expression in human blood cells by a third-generation lentiviral vector. *Gene Ther*. 2003;10(17):1446–1457.
59. Nagata K, Ohtani K, Nakamura M, Sugamura K. Activation of endogenous c-fos proto-oncogene expression by human T-cell leukemia virus type I-encoded p40tax protein in the human T-cell line, Jurkat. *J Virol*. 1989;63(8):3220–3226.
60. Dull T, et al. A third-generation lentivirus vector with a conditional packaging system. *J Virol*. 1998;72(11):8463–8471.
61. Shin HJ, Lee JB, Park SH, Chang J, Lee CW. T-bet expression is regulated by EGR1-mediated signaling in activated T cells. *Clin Immunol*. 2009;131(3):385–394.

MAJOR ARTICLE

Mogamulizumab, an Anti-CCR4 Antibody, Targets Human T-Lymphotropic Virus Type 1–infected CD8$^+$ and CD4$^+$ T Cells to Treat Associated Myelopathy

Junji Yamauchi,[1,2] Ariella Coler-Reilly,[1] Tomoo Sato,[1] Natsumi Araya,[1] Naoko Yagishita,[1] Hitoshi Ando,[1] Yasuo Kunitomo,[1] Katsunori Takahashi,[1] Yuetsu Tanaka,[4] Yugo Shibagaki,[2] Kusuki Nishioka,[5] Toshihiro Nakajima,[5] Yasuhiro Hasegawa,[3] Atae Utsunomiya,[6] Kenjiro Kimura,[2] and Yoshihisa Yamano[1]

[1]Department of Rare Diseases Research, Institute of Medical Science, [2]Division of Nephrology and Hypertension, [3]Division of Neurology, Department of Internal Medicine, St. Marianna University School of Medicine, Kawasaki, [4]Department of Immunology, Graduate School of Medicine, University of the Ryukyus, Okinawa, [5]Institute of Medical Science, Tokyo Medical University, and [6]Department of Hematology, Imamura Bun-in Hospital, Kagoshima, Japan

Background. Human T-lymphotropic virus type 1 (HTLV-1) can cause chronic spinal cord inflammation, known as HTLV-1–associated myelopathy/tropical spastic paraparesis (HAM/TSP). Since CD4$^+$CCR4$^+$ T cells are the main HTLV-1 reservoir, we evaluated the defucosylated humanized anti-CCR4 antibody mogamulizumab as a treatment for HAM/TSP.

Methods. We assessed the effects of mogamulizumab on peripheral blood mononuclear cells from 11 patients with HAM/TSP. We also studied how CD8$^+$ T cells, namely CD8$^+$ CCR4$^+$ T cells and cytotoxic T lymphocytes, are involved in HTLV-1 infection and HAM/TSP pathogenesis and how they would be affected by mogamulizumab.

Results. Mogamulizumab effectively reduced the HTLV-1 proviral load (56.4% mean reduction at a minimum effective concentration of 0.01 μg/mL), spontaneous proliferation, and production of proinflammatory cytokines, including interferon γ (IFN-γ). Like CD4$^+$CCR4$^+$ T cells, CD8$^+$CCR4$^+$ T cells from patients with HAM/TSP exhibited high proviral loads and spontaneous IFN-γ production, unlike their CCR4$^-$ counterparts. CD8$^+$CCR4$^+$ T cells from patients with HAM/TSP contained more IFN-γ–expressing cells and fewer interleukin 4–expressing cells than those from healthy donors. Notably, Tax-specific cytotoxic T lymphocytes that may help control the HTLV-1 infection were overwhelmingly CCR4$^-$.

Conclusions. We determined that CD8$^+$CCR4$^+$ T cells and CD4$^+$CCR4$^+$ T cells are prime therapeutic targets for treating HAM/TSP and propose mogamulizumab as a new treatment.

Keywords. HTLV-1; HAM/TSP; CCR4; mogamulizumab; CD8.

Human T-lymphotropic virus type 1 (HTLV-1) infects 10–20 million people worldwide, causing HTLV-1–associated myelopathy/tropical spastic paraparesis (HAM/TSP) and adult T-cell leukemia/lymphoma (ATL) in a small fraction of infected individuals [1–3]. HAM/TSP is an inflammatory disease of the central nervous system (CNS) that is thought to develop via so-called bystander damage, meaning that the host immune responses to HTLV-1–infected cells in the CNS damage the spinal cord [4]. Currently established treatments for HAM/TSP, such as corticosteroids [5] and interferon alfa [6], do not effectively reduce the HTLV-1 proviral load, which is well correlated with disease severity [7]. Reverse transcriptase inhibitors, which are used against human immunodeficiency virus type 1, were not effective against HTLV-1 in

Received 6 May 2014; accepted 28 July 2014; electronically published 7 August 2014.

Correspondence: Yoshihisa Yamano, MD, PhD, Department of Rare Diseases Research, Institute of Medical Science, St. Marianna University School of Medicine, 2-16-1, Sugao, Miyamae-ku, Kawasaki, Kanagawa 216-8512, Japan (yyamano@marianna-u.ac.jp).

The Journal of Infectious Diseases® 2015;211:238–48

DOI: 10.1093/infdis/jiu438

clinical trials [8, 9]. These and other existing antiviral drugs usually block the viral replication process [10], but HTLV-1 may escape these drugs by replicating using host cell division [11, 12]. The ideal treatment strategy for HAM/TSP would be selectively targeting and eliminating the HTLV-1–infected cells, but no such treatments currently exist.

Mogamulizumab, a defucosylated humanized anti-CCR4 immunoglobulin G1 (IgG1) monoclonal antibody, was recently approved in Japan as a novel therapy for ATL [13]. Importantly, ATL cells usually express chemokine receptor CCR4 [14]. Mogamulizumab strongly binds to Fcγ receptor IIIa (FcγRIIIa) on natural killer (NK) cells and elicits powerful antibody-dependent cellular cytotoxicity (ADCC) against the $CCR4^+$ ATL cells [15, 16].

Recently, we found that $CD4^+CD25^+CCR4^+$ T cells are the main HTLV-1 reservoir in HAM/TSP [17]. These cells abnormally produce interferon γ (IFN-γ) and are thought to play an important role in producing the chronic inflammation in HAM/TSP [17]. Thus, we began investigating the possibility of treating HAM/TSP and ATL by targeting $CCR4^+$ cells. We have already established that the defucosylated human/mouse chimeric anti-CCR4 antibody KM2760 effectively reduces the HTLV-1 proviral load in cultured peripheral blood mononuclear cells (PBMCs) from patients with HAM/TSP [18]. Here, we evaluate for the first time the effects of the humanized antibody mogamulizumab on cells from patients with HAM/TSP.

There is a population of $CD8^+$ T cells that express CCR4, but these cells have so far received much less attention than $CD4^+$ $CCR4^+$ T cells from HTLV-1 researchers. Although it has been shown that HTLV-1 infects $CD8^+$ T cells [19], it is as of yet unknown which among $CD8^+$ T cells are predominantly infected, as well as whether and how the infection influences the functions of those cells. $CD8^+CCR4^+$ T cells are reported to suppress inflammation and play a beneficial role in controlling chronic inflammatory diseases [20, 21]. It is important to determine whether $CD8^+CCR4^+$ T cells are protective or harmful during HAM/TSP pathogenesis, as well as how these cells would be affected by mogamulizumab.

We hypothesized that $CCR4^+$ cells among $CD8^+$ and $CD4^+$ T cells are highly infected and liable to develop proinflammatory traits. It has been reported that HTLV-1 preferentially transmits to $CCR4^+$ T cells through CCL22 (a CCR4 ligand) production induced by the HTLV-1 protein product Tax [22]. Tax has also been reported to induce IFN-γ production via transcriptional alterations within the infected cells themselves [18].

In the present study, we determined that mogamulizumab is effective at reducing the proviral load and proinflammatory character in PBMCs from patients with HAM/TSP. Next, we revealed that $CD8^+CCR4^+$ T cells are indeed highly infected by HTLV-1 and become proinflammatory. Finally, we determined that the majority of Tax-specific cytotoxic T lymphocytes (CTLs) were $CCR4^-$, indicating that they would not be inadvertently targeted by mogamulizumab. Our results indicate that $CD8^+CCR4^+$ T cells should be considered a key therapeutic target when developing treatments for HAM/TSP and that mogamulizumab represents a viable candidate for such a treatment.

METHODS

Subjects

This study was approved by the Institutional Ethics Committee at St. Marianna University and conducted in compliance with the Declaration of Helsinki. All participants gave written informed consent. Blood samples were obtained from 11 patients with HAM/TSP (8 females and 3 males; median age, 57 years [range, 47–72 years]; proviral load, 4.7 copies/100 cells [range, 1.26–9.71 copies/100 cells]), 8 HTLV-1–positive asymptomatic carriers (6 females and 2 males; median age, 57 years [range, 28–76 years]; proviral load, 4.7 copies/100 cells [range, 2.43–13.19 copies/100 cells]), and 8 HTLV-1–negative healthy volunteers (6 females and 2 males; median age, 59 years [range, 51–72 years]). HTLV-1 seropositivity was determined by a particle agglutination assay (Fujirebio, Tokyo, Japan) and confirmed by Western blot (SRL Inc., Tokyo, Japan). HAM/TSP was diagnosed according to the World Health Organization guidelines [23]. PBMCs were separated by Ficoll-Hypaque density gradient centrifugation (Pancoll; PAN-Biotech, Aidenbach, Germany) and viably cryopreserved in liquid nitrogen with freezing medium (Cell Banker 1; Mitsubishi Chemical Medience Corporation, Tokyo, Japan).

Cell Culture

PBMCs were seeded at 1×10^5 cells/200 μL/well in 96-well round-bottomed plates in the presence or absence of mogamulizumab or KM2760 (gifts from Kyowa Hakko Kirin Co., Ltd., Tokyo, Japan) or human control IgG (Jackson ImmunoResearch Laboratories, West Grove, PA) or prednisolone (LKT Laboratories, Inc., St. Paul, MN) and incubated at 37°C in 5% CO_2. Roswell Park Memorial Institute 1640 medium was supplemented with 10% heat-inactivated fetal bovine serum and 1% penicillin and streptomycin antibiotic solution (Wako Pure Chemical Industries Ltd., Osaka, Japan). The supernatants were collected and stored at −80°C. The cells were harvested for DNA extraction or fluorescence-activated cell-sorter (FACS) analysis. The HTLV-1 proviral load was measured using ABI Prism 7500 SDS (Applied Biosystems, Carlsbad, CA), as described previously [24].

Cell Proliferation Assay

PBMCs from patients with HAM/TSP were cultured for 7 days as described above. PBMCs from healthy donors were stimulated with 4 μg/mL of phytohemagglutinin-P (PHA; Sigma-Aldrich, St. Louis, MO) and cultured in the presence or absence of mogamulizumab or prednisolone for 3 days. During the last 16 hours, 1 μCi of ^{3}H-thymidine was added to each well, and then cells were harvested and counted with a β-plate counter (Wallac-Perkin Elmer, Waltham, MA). The assay was performed in triplicate, and average values were used for analysis.

Measurement of Cytokines

The concentrations of 6 cytokines (IFN-γ, interleukin 2 [IL-2], interleukin 4 [IL-4], interleukin 6 [IL-6], interleukin 10 [IL-10], and tumor necrosis factor α [TNF-α]) in culture supernatants were measured with a cytometric bead array kit (BD Biosciences, San Diego, CA), using a FACSCalibur flow cytometer (BD Biosciences).

Flow Cytometric Analysis

Cells were immunostained with various combinations of the following fluorescence-conjugated antibodies to surface antigens: anti-CD3 (UCHT1), anti-CD4 (RPA-T4), anti-CD8 (RPA-T8), anti-CD14 (61D3), and anti-CD19 (HIB19), from eBiosciences (San Diego, CA); and anti-CD56 (B159) anti-CCR4 (1G1), from BD Biosciences. The epitope of the anti-CCR4 antibody (1G1) is different from that of mogamulizumab and KM2760, and thus these treatments do not affect the binding of 1G1 to CCR4 [16]. In some experiments, allophycocyanin-conjugated HLA-A*2402/HTLV-1 Tax301-309 tetramer (Medical & Biological Laboratories, Nagoya, Japan) was used. To identify HTLV-1–infected cells, cells were fixed and permeabilized using a staining buffer set (eBiosciences) and then intracellularly stained with anti-Tax antibody (Lt-4) [25]. To analyze intracellular effector molecules, cells were fixed and stained with the antibodies to perforin (δG9) and granzyme B (GB11; BD Biosciences). For intracellular cytokine staining, PBMCs were stimulated for 6 hours with phorbol 12-myristate 13-acetate (50 ng/mL) and ionomycin (1 μg/mL, Sigma-Aldrich Japan, Tokyo, Japan) in the presence of monensin (GolgiStop, BD Biosciences). After being harvested, the cells were fixed and stained with the antibodies to IFN-γ (B27) and IL-4 (MP4-25D2; BD Biosciences). The stained cells were analyzed using FACSCalibur, and the data were processed using FlowJo software (TreeStar, San Diego, CA). For cell sorting, $CD8^+$ T cells were negatively selected from PBMCs, using MACS beads (Miltenyi Biotec, Bergisch Gladbach, Germany). The purified $CD8^+$ T cells were stained with anti-CD3, anti-CD8, and anti-CCR4 antibodies, and then $CD3^+CD8^+$, $CD3^+CD8^+CCR4^+$, and $CD3^+CD8^+CCR4^-$ T cells were separated using a cell sorter (JSAN, Bay Bioscience Co., Ltd., Hyogo, Japan). The purity exceeded 95%.

Statistical Analysis

Values are expressed as means ± standard deviations. The paired *t* test or the Wilcoxon signed-rank test was used for within-group comparisons. The Mann–Whitney *U* test was used for comparisons between groups. Repeated-measures analysis of variance (ANOVA) followed by the Dunnett test or the Friedman test followed by the Dunn test were used for paired multiple comparisons. Statistical analyses were performed using GraphPad Prism 5 and Prism statistics (GraphPad Software, Inc., La Jolla, CA), and *P* values of <.05 were considered statistically significant.

RESULTS

Mogamulizumab and KM2760 Reduce the HTLV-1 Proviral Load and Inhibit Spontaneous Proliferation of PBMCs From Patients With HAM/TSP

The effects of mogamulizumab and KM2760 were assessed by measuring proviral loads in treated PBMCs from patients with HAM/TSP. ^{3}H-thymidine incorporation was used to assess the inhibitory effects of the antibodies on spontaneous cell proliferation, a distinctive phenomenon associated with PBMCs from HTLV-1–infected individuals by which the cells proliferate without mitogens or stimuli in vitro [26]. Mogamulizumab and KM2760 both reduced proviral load in a dose-dependent manner at concentrations of ≥0.01 μg/mL (mean reduction [±SD], 56.4% ± 21.1% and 61.1% ± 17.0%, respectively; $P < .01$ and $P < .001$, respectively; Figure 1*A*). Notably, there was a mean reduction (±SD) of 66.4% ± 20.2% in the proviral load with 10 μg/mL mogamulizumab ($P < .001$), which is the blood concentration of the antibody in patients with ATL treated with 1 mg/kg mogamulizumab [13]. Mogamulizumab and KM2760 similarly inhibited spontaneous proliferation in a dose-dependent manner at concentrations of ≥0.01 μg/mL (mean inhibition [±SD], 25.6% ± 31.9% and 22.1% ± 35.9%, respectively; $P < .01$ and $P < .05$, respectively; Figure 1*B*). Because mogamulizumab and KM2760 showed such similar results, only mogamulizumab was used in the next experiments as representative of the 2. Mogamulizumab was also tested against human IgG to control for nonspecific antibody effects and more effectively reduced the proviral load and spontaneous proliferation (Supplementary Figure 1*A* and 1*B*). Mogamulizumab reduced the HTLV-1 proviral load in cells from asymptomatic carriers, as well, in a dose-dependent manner (Figure 1*C*). Finally, mogamulizumab inhibited PHA-stimulated proliferation of PBMCs from healthy donors at concentrations of ≥0.1 μg/mL ($P < .01$), but the effects of prednisolone were much more pronounced than those of mogamulizumab (prednisolone vs mogamulizumab, $P < .001$; Figure 1*D*).

Prednisolone suppressed spontaneous proliferation (mean inhibition [±SD], 37.4% ± 35.2%; $P < .001$; Figure 1*B*) but did not decrease proviral load (Figure 1*A*). The combination of mogamulizumab and 0.1 μg/mL of prednisolone, which corresponds to the serum concentration achieved when 5 mg of prednisolone is administered orally [27], reduced proviral load as much as but no more than did mogamulizumab alone (Supplementary Figure 2*A*). On the other hand, ^{3}H-thymidine incorporation was substantially more inhibited by the combination treatment than with mogamulizumab alone (mean inhibition [±SD], 81.3% ± 18.3% vs 71.3% ± 19.3%; $P = .01$; Supplementary Figure 2*B*).

Mogamulizumab and KM2760 Inhibit Proinflammatory Cytokine Production in PBMCs From HAM/TSP Patients

Here we examined the effects of mogamulizumab and KM2760 on cytokine production in PBMCs from patients with HAM/

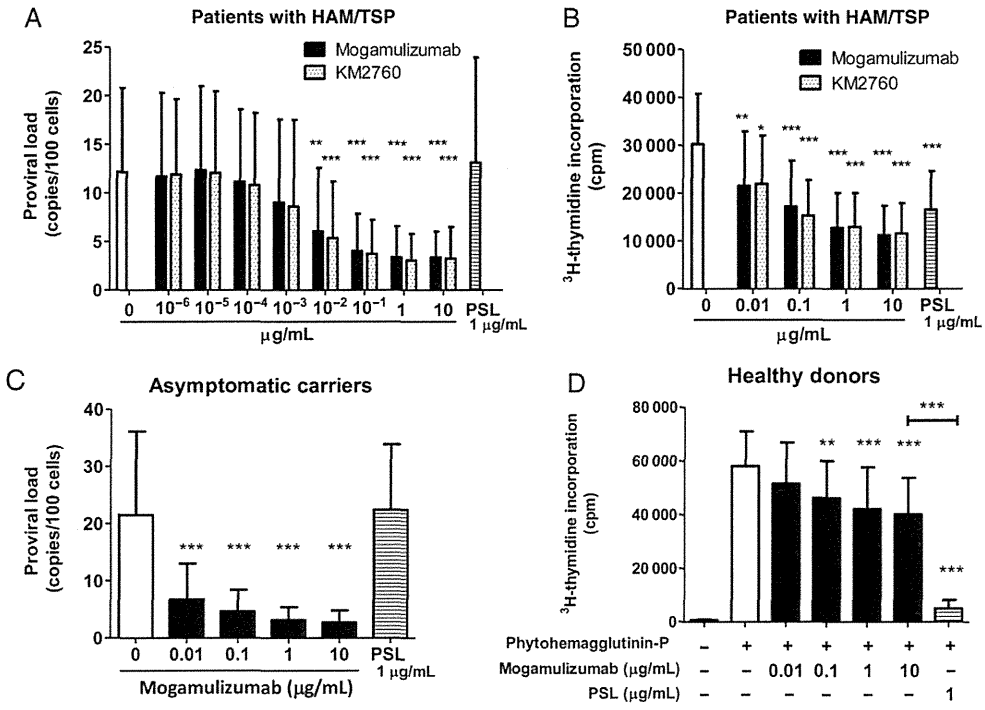

Figure 1. Mogamulizumab and KM2760 reduce the human T-lymphotropic virus type 1 (HTLV-1) proviral load and inhibit spontaneous proliferation of peripheral blood mononuclear cells (PBMCs) from patients with HTLV-1–associated myelopathy/tropical spastic paraparesis (HAM/TSP). *A* and *B*, PBMCs from 11 patients with HAM/TSP were cultured for 7 days without stimuli and without treatment or in the presence of mogamulizumab, KM2760, or prednisolone (PSL). Cells were harvested, and the proviral load was measured using real-time polymerase chain reaction (*A*). ^{3}H-thymidine was added during the last 16 hours of culturing. Cells were then harvested and analyzed for ^{3}H-thymidine incorporation (*B*). Because mogamulizumab and KM2760 were equally effective, only mogamulizumab was used thereafter as representative of the 2. *C*, PBMCs from 8 asymptomatic carriers were cultured for 7 days without treatment or in the presence of mogamulizumab or PSL, and the proviral load was measured as described above. *D*, PBMCs from 8 healthy donors were stimulated with 4 μg/mL of phytohemagglutinin-P and cultured for 3 days without treatment or in the presence of mogamulizumab or PSL. ^{3}H-thymidine incorporation was analyzed as described above. Data are presented as the mean ± SD. Statistical analyses were performed using repeated-measures analysis of variance, followed by the Dunnett test, for comparison with PBMCs alone (*A–C*) or with PBMCs stimulated with PHA (*D*). The paired *t* test was used to compare 10 μg/mL of mogamulizumab and PSL (*D*). **P* < .05, ***P* < .01, and ****P* < .001. Abbreviation: SD, standard deviation.

TSP. In line with previous reports [28], PBMCs produced various cytokines, most notably IFN-γ, in 7-day cultures without stimuli (Figure 2*A*). Mogamulizumab and KM2760 both reduced the production of the proinflammatory cytokines IFN-γ, IL-6, IL-2, and TNF-α, as well as the immunosuppressive cytokine IL-10 (Figure 2*B–F*). Mogamulizumab reduced IFN-γ production more than did human IgG (Supplementary Figure 1*C*). Prednisolone at a concentration of 1 μg/mL effectively reduced IFN-γ and TNF-α but not IL-2, IL-6, or IL-10 production.

Mogamulizumab Eliminates CCR4^{+} Cells Among Both CD4^{+} and CD8^{+} T cells

Mogamulizumab effectively eliminated the CD4^{+}CCR4^{+} T cells in cultured PBMCs from patients with HAM/TSP (Figure 3*A* and 3*B*). FACS analysis also revealed a population of CD4^{-} CCR4^{+} cells similarly affected by the antibody, and these cells were found to be CD8^{+} T cells (Figure 3*C*). Detailed investigation confirmed that CCR4^{+} T cells among the CD8^{+} subset were eliminated by mogamulizumab just as they were from the CD4^{+} subset (Figure 3*D–E*).

The ADCC Activity of Mogamulizumab Is Fast Acting and Specific

FACS analysis showed that mogamulizumab reduced the frequency of CCR4^{+} T cells among both CD4^{+} and CD8^{+} subsets within 6 hours ($P = .0003$ and $P = .004$, respectively), with a similar reduction in Tax^{+} T cells observed within 24 hours ($P = .01$ and $P = .03$, respectively; Figure 4*A–C* and Supplementary Figure 3). By contrast, mogamulizumab did not reduce the frequency of B cells, NK cells, or monocytes after 24 hours (Figure 4*D*).

CD8^{+}CCR4^{+} T Cells From Patients With HAM/TSP Are Numerous and Highly Infected by HTLV-1

CD8^{+}CCR4^{+} T cells were then further analyzed to assess their role in HAM/TSP and predict the potential benefits and risks of eradicating them with mogamulizumab. Samples from patients with HAM/TSP, compared with those from age-matched healthy donors, contained a higher proportion of CCR4^{+} cells among both the CD4^{+} T-cell subset ($P = .003$) and the CD8^{+} T-cell subset ($P = .02$; Figure 5*A*). In addition, the proviral

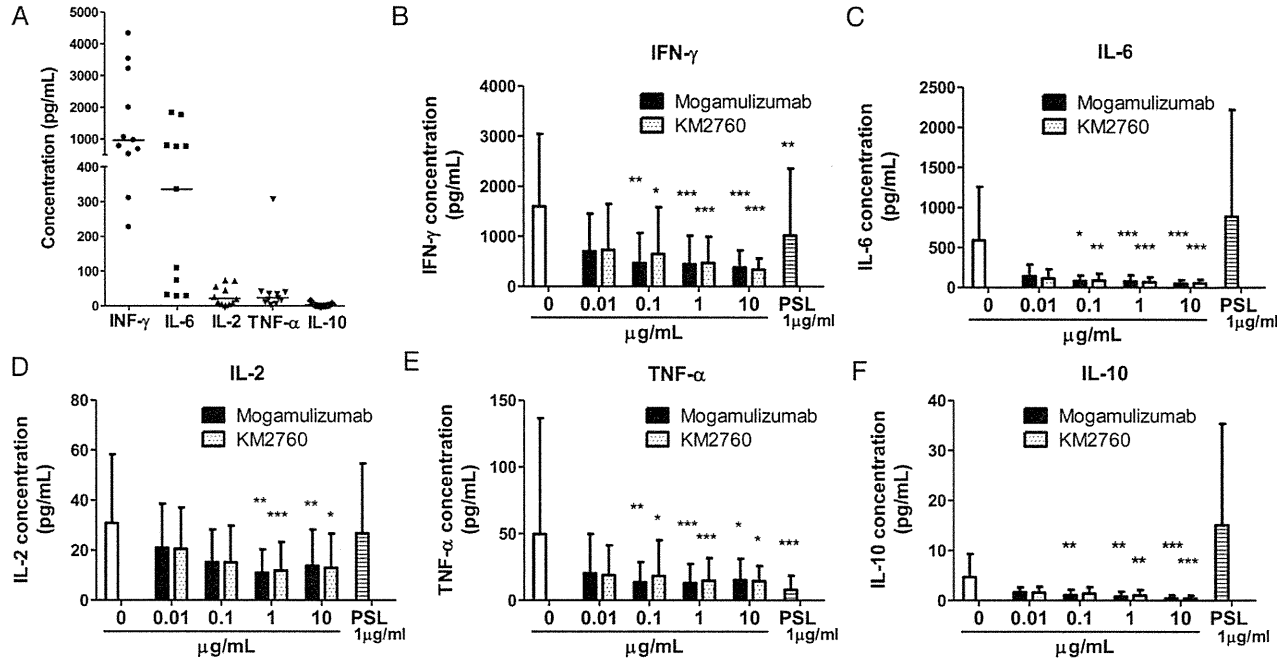

Figure 2. Mogamulizumab and KM2760 inhibit cytokine production in peripheral blood mononuclear cells (PBMCs) from patients with human T-lymphotropic virus type 1–associated myelopathy/tropical spastic paraparesis (HAM/TSP). PBMCs from 11 patients with HAM/TSP were cultured for 7 days without stimuli and without treatment or in the presence of mogamulizumab, KM2760, or prednisolone (PSL). The concentrations of cytokines (interferon γ [IFN-γ], interleukin 6 [IL-6], interleukin 2 [IL-2], tumor necrosis factor α [TNF-α], and interleukin 10 [IL-10]) in the supernatants were then measured. *A*, Direct comparison of the concentrations of these cytokines in the supernatants of untreated PBMC cultures. Horizontal bars represent the median values. *B–F*, The effects of the treatments on the concentrations of these cytokines. Data are presented as the mean ± SD. Statistical analyses were performed using the Friedman test followed by the Dunn test for comparison with PBMCs alone. **P* < .05, ***P* < .01, and ****P* < .001. Abbreviation: SD, standard deviation.

load was significantly higher in $CD8^+CCR4^+$ T cells than in $CD8^+CCR4^-$ T cells (mean load [±SD], 13.6 ± 7.9 copies/100 cells and 0.72 ± 0.65 copies/100 cells, respectively; $P = .0002$; Figure 5*B*).

$CD8^+CCR4^+$ T Cells From Patients With HAM/TSP Possess Proinflammatory Properties

Here we investigated the functional differences between $CD8^+CCR4^+$ T cells from patients with HAM/TSP and those from healthy donors. $CD8^+CCR4^+$ cells from both groups expressed minimal perforin and granzyme B (Figure 5*C* and 5*D*). In the $CD8^+CCR4^-$ T-cell subset, the frequency of perforin-expressing cells was unremarkable, but the frequency of granzyme B–expressing cells was higher in patients with HAM/TSP than in healthy donors ($P = .04$; Figure 5*C* and 5*D*). Next, cytokine expression was evaluated in PBMCs stimulated with phorbol 12-myristate 13-acetate and ionomycin in the presence of monensin. Interestingly, samples from patients with HAM/TSP included more IFN-γ–producing cells ($P = .02$; Figure 5*E*) but fewer IL-4–producing cells ($P = .01$; Figure 5*F*) in the $CD8^+CCR4^+$ T-cell subset than did samples from healthy donors. On the other hand, there were no such significant differences among $CD8^+CCR4^-$ T cells (Figure 5*E* and 5*F*). Finally, the concentrations of cytokines in the supernatants of unstimulated cultures of isolated total $CD8^+$, $CD8^+CCR4^-$, and $CD8^+CCR4^+$ T cells were measured to assess spontaneous cytokine production in these cell populations. Spontaneous IFN-γ production, like spontaneous proliferation, is a hallmark of PBMCs from patients with HAM/TSP [29,30]. Unsurprisingly, IFN-γ was detected in no cell population from healthy donors. Among samples from patients with HAM/TSP, $CD8^+CCR4^+$ T cells produced remarkably more IFN-γ than did $CD8^+CCR4^-$ cells (mean level [±SD], 364.0 ± 445.3 pg/mL vs 1.9 ± 4.5 pg/mL; $P = .001$; Figure 5*G*). IL-4 was not detected in any of the samples (data not shown).

The Majority of HTLV-1 Tax-Specific Cytotoxic T Lymphocytes Are $CCR4^-$

We analyzed CCR4 expression in Tax-specific CTLs to determine whether CTLs against HTLV-1 also become targets of mogamulizumab. Among the 11 patients studied, 7 had HLA-A*2402 and were analyzed using the HLA-A*2402/HTLV-1 Tax301-309 tetramer. The majority of Tax-specific CTLs did not express CCR4, and the percentage of $CCR4^+$ cells was lower in CTLs than in total $CD8^+$ T cells (mean frequency [±SD], 2.3% ± 1.0% and 8.5 ± 4.7%, respectively; $P = .02$; Figure 6).

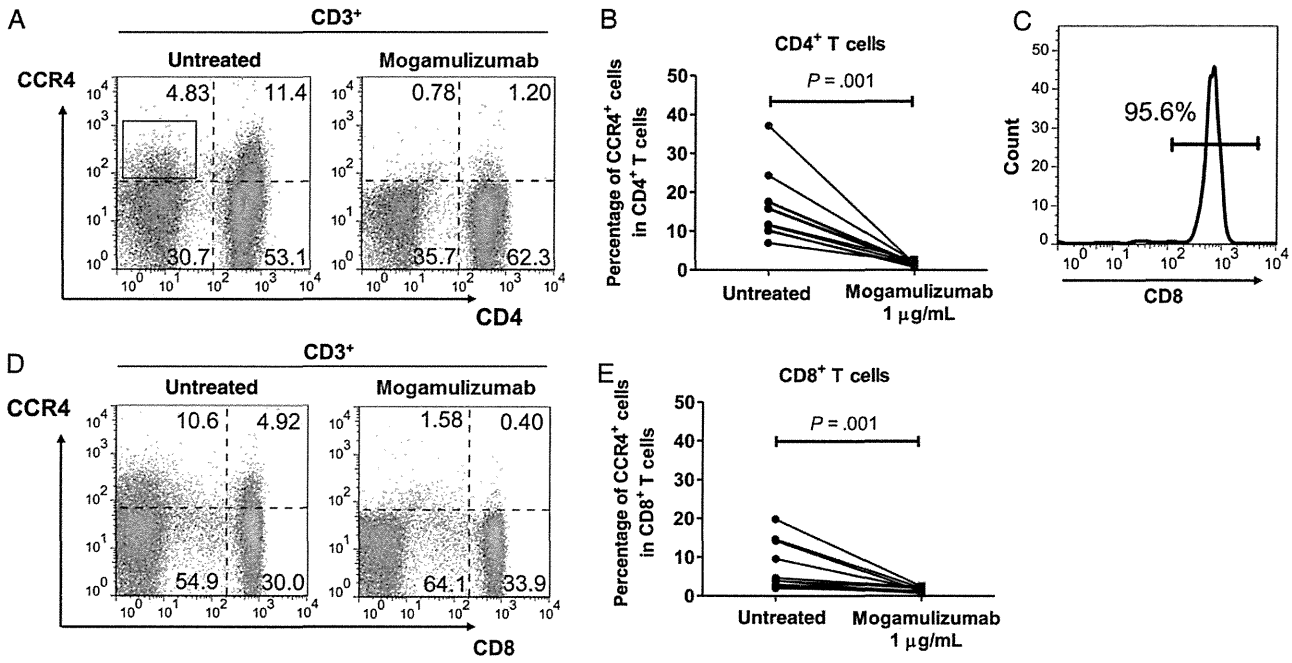

Figure 3. Mogamulizumab eliminates CCR4$^+$ cells in both CD4$^+$ and CD8$^+$ T cells. *A*, Representative dot plots of fluorescence-activated cell-sorter analysis of CCR4 and CD4 expression in CD3$^+$ T cells among peripheral blood mononuclear cells from patients with human T-lymphotropic virus type 1–associated myelopathy/tropical spastic paraparesis after 5-day culture in the presence or absence of 1 μg/mL of mogamulizumab. *B*, Percentages of CCR4$^+$ cells in CD3$^+$CD4$^+$ T cells were compared between the untreated and mogamulizumab groups (n = 11). Statistical analysis was performed using the Wilcoxon signed-rank test. *C*, The population enclosed in the box in panel *A* (the CD3$^+$CD4$^-$CCR4$^+$ subset) was gated and analyzed for the expression of CD8. The percentage of CD8$^+$ cells is shown. *D* and *E*, CCR4 and CD8 expression in CD3$^+$ T cells was analyzed as described above.

DISCUSSION

In this study, we established mogamulizumab as a novel candidate treatment for HAM/TSP that targets infected cells by marking CCR4$^+$ T cells for elimination. Mogamulizumab reduced the number of infected cells, as measured via the proviral load, and thus inhibited the excessive immune responses such as spontaneous proliferation and proinflammatory cytokine production that are attributed to those infected cells (Figures 1 and 2). Effects of mogamulizumab-induced ADCC activity were detectable by FACS after as little as 6 hours of culturing (Figure 4*A*–*C*).

The remaining proviral load after mogamulizumab therapy was higher than expected (mean load [±SD], 3.25 ± 2.58 copies/100 cells; Figure 1*A*). CD4$^+$CCR4$^-$ T cells [18] and CD8$^+$CCR4$^-$ T cells (Figure 5*B*) from patients with HAM/TSP were predominantly uninfected, and the antibody therapy should have destroyed the vast majority of the infected CCR4$^+$ T cells (Figure 3), yielding an expected proviral load of <1.0 copy/100 cells. It is possible that some CCR4$^-$ T cells became infected while the samples were being cultured, which is a potential limitation of such in vitro experiments.

The inhibitory effects of mogamulizumab on PHA-stimulated proliferation in PBMCs from healthy donors were statistically significant but still minimal, compared with those of prednisolone (Figure 1*D*), indicating that mogamulizumab, in contrast to immunosuppressive agents, acts via specific reduction of infected cells rather than via nonspecific immune suppression. Interestingly, prednisolone was considerably less effective at suppressing the proliferation of T cells from patients with HAM/TSP (Figure 1*B*) than from healthy donors. Although we cannot be sure of the reasons behind this discrimination, it appears that spontaneous proliferation is less vulnerable to suppression by steroids since it is not a simple T-cell response to antigens [31, 32]. Nevertheless, compared with mogamulizumab alone, the combination with prednisolone enhanced the suppressive effect of mogamulizumab on spontaneous proliferation without hampering proviral load reduction (Supplementary Figure 2).

Mogamulizumab also reduced the proviral load in PBMCs from asymptomatic carriers (Figure 1*C*), which suggests that it can be administered as a preventive treatment to asymptomatic carriers with high proviral loads who are at risk for developing HAM/TSP or ATL. It is well established that high proviral load is associated with the onset and progression of HAM/TSP [7, 33], as well as with the development of ATL [34].

It was well known that although the main reservoir for HTLV-1 is CD4$^+$ T cells, the virus also infects CD8$^+$ T cells in patients

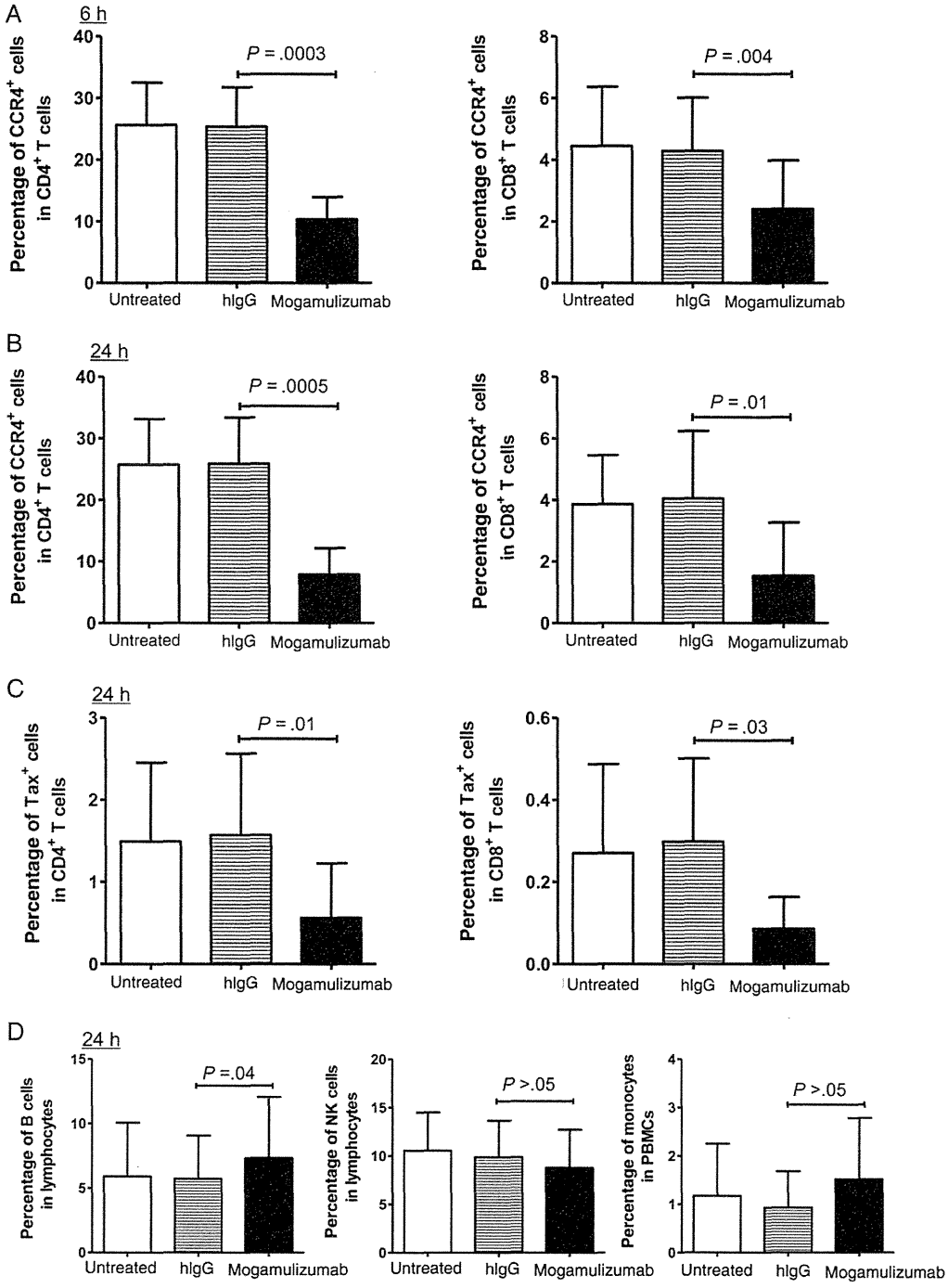

Figure 4. The antibody-dependent cellular cytotoxicity activity of mogamulizumab is fast acting and specific. Peripheral blood mononuclear cells (PBMCs) from 6 patients with human T-lymphotropic virus type–associated myelopathy/tropical spastic paraparesis were cultured in the presence of 1 μg/mL of mogamulizumab or human immunoglobulin G (hIgG) or without treatment. $CD4^+$ and $CD8^+$ T cells were analyzed using fluorescence-activated cell-sorter analysis, and the frequencies of $CCR4^+$ cells after 6 hours (*A*) and 24 hours (*B*), as well as that of Tax^+ cells (*C*) after 24 hours, are shown here. The frequencies of $CD19^+$ B cells and $CD3^-CD56^+$ natural killer (NK) cells among lymphocytes, as well as $CD14^+$ monocytes among PBMCs after 24 hours are also shown (*D*). Data are presented as the mean ± SD. The paired *t* test was used to compare the effects of mogamulizumab and hIgG. Abbreviation: SD, standard deviation.

with HAM/TSP [19]. Here we revealed for the first time that the overwhelming majority of infected $CD8^+$ T cells also expressed CCR4 (Figure 5*B*). Our findings in this study suggest that it is important to eliminate both $CD4^+CCR4^+$ and $CD8^+CCR4^+$ T-cell subsets because both have elevated proviral loads and a tendency to develop proinflammatory traits (Figure 5).

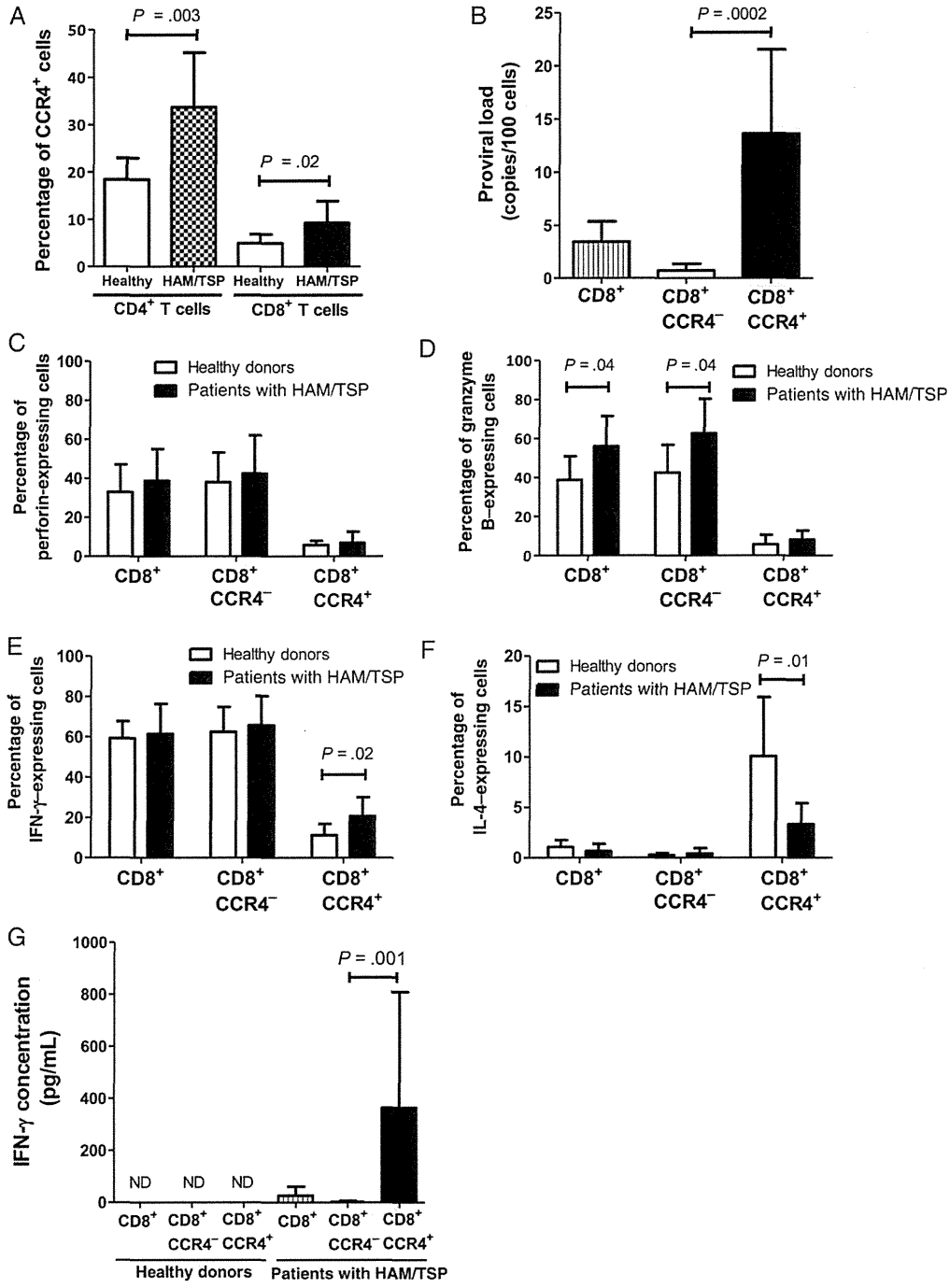

Figure 5. $CD8^+CCR4^+$ T cells from patients with human T-lymphotropic virus type 1 (HTLV-1)–associated myelopathy/tropical spastic paraparesis (HAM/TSP) are numerous, highly HTLV-1 infected, and proinflammatory. *A*, Proportions of $CCR4^+$ cells among $CD4^+$ and $CD8^+$ T cells in 8 healthy donors and 11 patients with HAM/TSP were analyzed by fluorescence-activated cell-sorter (FACS) analysis. *B*, The HTLV-1 proviral load in total $CD3^+CD8^+$, $CD3^+CD8^+CCR4^-$, and $CD3^+CD8^+CCR4^+$ T-cell subsets. $CD8^+$ T cells from 11 patients with HAM/TSP were isolated using negative separation with magnetic beads, and then $CD3^+CD8^+$, $CD3^+CD8^+CCR4^-$ and $CD3^+CD8^+CCR4^+$ T cells were separated with FACS analysis. Proviral loads in each subset were measured using real-time polymerase chain reaction. *C–F*, Peripheral blood mononuclear cells (PBMCs) from 8 healthy donors and 11 patients with HAM/TSP were stained for CD8 and CCR4, as well as intracellular perforin or granzyme B, and analyzed using FACS analysis. PBMCs from the same individuals were stimulated with phorbol 12-myristate 13-acetate (50 ng/mL) and ionomycin (1 μg/mL) in the presence of monensin for 6 hours. The cells were then analyzed for CD8, CCR4, and intracellular interferon γ (IFN-γ) or interleukin 4 (IL-4) expressions. The percentages of perforin-expressing (*C*), granzyme B–expressing (*D*), IFN-γ–expressing (*E*), and IL-4–expressing (*F*) cells in total $CD8^+$, $CD8^+CCR4^-$, and $CD8^+CCR4^+$ T-cell subsets from healthy donors versus patients with HAM/TSP are shown. *P* values are indicated only when <.05. *G*, $CD3^+CD8^+$, $CD3^+CD8^+CCR4^-$, and $CD3^+CD8^+CCR4^+$ T cells were isolated from 6 healthy donors and 11 patients with HAM/TSP as described above. These cells (3×10^4 cells/well) were cultured for 3 days without stimuli, and the concentration of IFN-γ in the supernatants was measured. Statistical analysis was performed using the Mann–Whitney *U*-test (*A* and *C–F*) or the Wilcoxon signed-rank test (*B* and *G*). Data are presented as the mean ± SD. Abbreviation: SD, standard deviation.

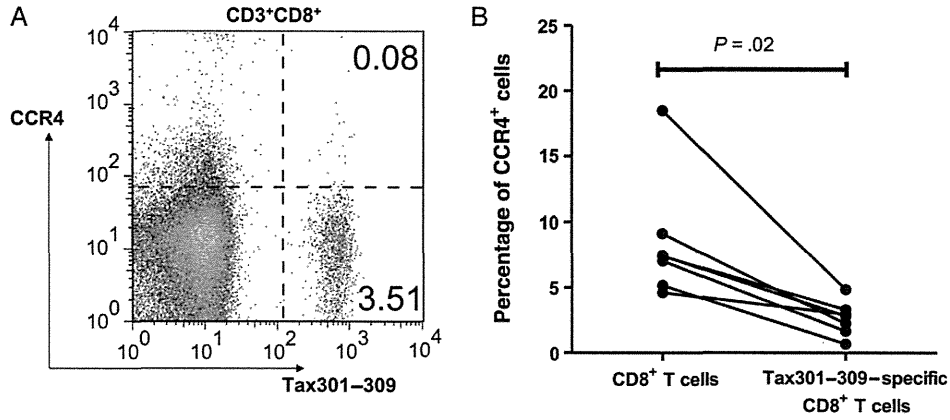

Figure 6. $CD8^+CCR4^+$ T cells from patients with human T-lymphotropic virus type 1 (HTLV-1)–associated myelopathy/tropical spastic paraparesis (HAM/TSP) do not include many Tax-specific cytotoxic T lymphocytes (CTLs). *A*, A representative dot plot of fluorescence-activated cell-sorter (FACS) analysis of the expression of CCR4 in HTLV-1 Tax-specific CTLs. Peripheral blood mononuclear cells from a patient with HAM/TSP and HLA-A*2402 were stained with antibodies for CD3, CD8, CCR4, and HLA-A*2402-restricted Tax301-309–specific tetramer. The $CD3^+CD8^+$ subset was gated. The values in the upper and lower right quadrants indicate the percentages of $CCR4^+$ and $CCR4^-$ Tax-specific CTLs among $CD3^+CD8^+$ T cells, respectively. *B*, Proportions of $CCR4^+$ cells among total $CD8^+$ T cells and Tax301-309–specific $CD8^+$ T cells are compared (n = 7). Statistical analysis was performed using the Wilcoxon signed-rank test.

$CD8^+CCR4^+$ T cells normally produce IL-4 more often than IFN-γ and hardly produce any cytotoxic granules [35, 36]; these cells are thought to be protective against type 1-skewed inflammation [21, 37]. In patients with HAM/TSP, these $CD8^+CCR4^+$ but not $CD8^+CCR4^-$ T cells are altered to produce IFN-γ rather than IL-4 (Figure 5*E* and 5*F*). $CD8^+CCR4^+$ T cells cultured alone exhibited spontaneous IFN-γ production (Figure 5*G*), a hallmark of PBMCs from patients with HAM/TSP [29, 30]. These results suggest that abnormal cells contributing to the pathogenesis of HAM/TSP exist not only among $CD4^+CCR4^+$ T cells but also among $CD8^+CCR4^+$ T cells. It is thought that the functional abnormalities of these cells may arise through transformations occurring within the infected cells themselves, whereby HTLV-1 Tax induces transcriptional alterations via T box transcription factor [18].

In the present study, HTLV-1 infection did not influence cytotoxic granule production in $CD8^+CCR4^+$ T cells (Figure 5*C* and 5*D*). The slightly increased fraction of granzyme B^+ cells in $CD8^+CCR4^-$ T cells from patients with HAM/TSP is presumably attributable to the immune activation resulting from the chronic viral infection [38–40].

Although eliminating the abnormal immune responses of the infected cells should alleviate inflammation and related symptoms of the infection, it is also true that immune responses against HTLV-1 are important for controlling said infection [41]. We evaluated CCR4 expression in HTLV-1 Tax-specific CTLs for fear that use of mogamulizumab might inadvertently destroy CTLs that would have helped to control the infection [42, 43]. Since Tax-specific CTLs have been reported to be preferentially infected by HTLV-1 [44], there was some concern that our finding that infected $CD8^+$ T cells are predominantly $CCR4^+$ meant that these CTLs would also be targeted by mogamulizumab. However, we found that the majority of Tax-specific CTLs do not express CCR4 (Figure 6), meaning that they should essentially be spared during mogamulizumab treatment.

Also concerning is that mogamulizumab is expected to target $CD4^+CCR4^+$ regulatory T (Treg) cells [45], which could elicit autoimmune problems and even exacerbate the chronic inflammation plaguing patients with HAM/TSP. However, there are also $CCR4^-$ Treg cells [45], which would be spared, and there have been no reports of increased incidence of autoimmune disease in patients with ATL treated with mogamulizumab. Furthermore, reducing the number of Treg cells may benefit patients with HAM/TSP by preventing abundant Treg cells from dampening immune control of the HTLV-1 infection [28, 46].

We expect that eliminating HTLV-1–infected cells in the peripheral blood with mogamulizumab would reduce the number of proinflammatory cells and mitigate the inflammation in the CNS. Although HAM/TSP is a disease of the CNS, recent reports suggest that it is indeed effective to target HTLV-1–infected cells in the peripheral blood because continued migration of infected cells from the peripheral blood maintains and even exacerbates the inflammation in the CNS [30].

Based on the results of this study, we have begun conducting a clinical trial to test the efficacy of mogamulizumab on patients with HAM/TSP (UMIN000012655). Our data suggest that as little as one thousandth of the dose administered to patients with ATL (1 mg/kg body weight [13]) may be effective for patients with HAM/TSP. In contrast to patients with an aggressive cancer such as ATL, those with a chronic inflammatory disorder like HAM/TSP would benefit from a more conservative approach that is safer but still effective.